

000  
001  
002  
003  
004  
005  
006  
007  
008

# AutoDrive- $P^3$ : UNIFIED CHAIN OF PERCEPTION–PREDICTION–PLANNING THOUGHT VIA REINFORCEMENT FINE-TUNING

009  
010  
011  
012  
013  
014**Anonymous authors**

Paper under double-blind review

## ABSTRACT

015  
016  
017  
018  
019  
020  
021  
022  
023  
024  
025  
026  
027  
028  
029  
030  
031  
032  
033  
034  
035  
036  
037

Vision-language models (VLMs) are increasingly being adopted for end-to-end autonomous driving systems due to their exceptional performance in handling long-tail scenarios. However, current VLM-based approaches suffer from two major limitations: 1) Some VLMs directly output planning results without chain-of-thought (CoT) reasoning, bypassing crucial perception and prediction stages which creates a significant domain gap and compromises decision-making capability; 2) Other VLMs can generate outputs for perception, prediction, and planning tasks but employ a fragmented decision-making approach where these modules operate separately, leading to a significant lack of synergy that undermines true planning performance. To address these limitations, we propose *AutoDrive- $P^3$* , a novel framework that seamlessly integrates Perception, Prediction, and Planning through structured reasoning. We introduce the  $P^3$ -CoT dataset to facilitate coherent reasoning and propose  $P^3$ -GRPO, a hierarchical reinforcement learning algorithm that provides progressive supervision across all three tasks. Specifically, *AutoDrive- $P^3$*  progressively generates CoT reasoning and answers for perception, prediction, and planning, where perception provides essential information for subsequent prediction and planning, while both perception and prediction collectively contribute to the final planning decisions, enabling safer and more interpretable autonomous driving. **Additionally, to balance inference efficiency with performance, we introduce dual thinking modes: detailed thinking and fast thinking.** Extensive experiments on both open-loop (nuScenes) and closed-loop (NAVSIMv1/v2) benchmarks demonstrate that our approach achieves state-of-the-art performance in planning tasks.

038  
039

## 1 INTRODUCTION

040  
041  
042  
043  
044  
045  
046  
047  
048

Autonomous driving aims to predict trajectories that are both comfortable and collision-free by leveraging environmental and ego-vehicle information. Traditional approaches decouple the autonomous driving pipeline into three independent stages: perception (Li et al., 2024c; Liang et al., 2022), prediction (Zhou et al., 2023; Shi et al., 2024), and planning (Huang et al., 2024b; Liu et al., 2025). However, these module design often leads to error accumulation, which significantly degrades the final trajectory quality. Recent years have witnessed significant advancements in end-to-end training for autonomous systems (Hu et al., 2023; 2022; Jiang et al., 2023), as shown in Fig. 1(a). Nevertheless, these small-scale end-to-end models are constrained by limited dataset size and model capacity, resulting in a lack of world knowledge and poor performance in long-tail scenarios.

049  
050  
051  
052  
053

To address long-tail scenarios, recent works (Tian et al., 2024; Wang et al., 2024; Zhou et al., 2025a;b; Yuan et al., 2025) introduce Vision-Language Models (VLMs) into autonomous driving. Leveraging large-scale pre-training, VLMs show strong adaptability to diverse scenarios. However, current VLM-based end-to-end systems face three key limitations: **1) Lack of Chain-of-Thought (CoT) supervision:** VLM-based systems benefit from CoT, but some VLMs directly output trajectories (Fig. 1(b)), limiting reasoning for decision-making. **2) Lack of multi-task synergy:** Although

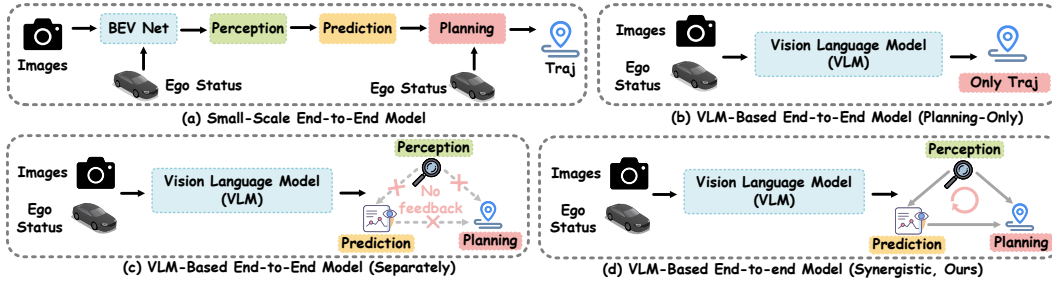


Figure 1: **The difference between *AutoDrive-P<sup>3</sup>* and other paradigms.** Our method combines an end-to-end training framework with a three-stage collaborative supervision form with VLM.

most VLMs (Zhou et al., 2025a; Wang et al., 2024) can answer perception, prediction, and planning queries (Fig. 1(c)), they treat these tasks separately, resulting in poor synergy and weak planning. **3) Planning-only GRPO supervision:** Existing Group Relative Policy Optimization (GRPO) applications optimize only planning metrics such as L2 distance or closed-loop performance (Zhou et al., 2025b; Yuan et al., 2025), leaving perception and prediction without direct supervision. This yields superficial gains, limited interpretability, and unreliable planning.

We argue that these limitations lies in the failure to capture the staged CoT process across perception, prediction, and planning. Autonomous driving fundamentally requires these three stages to work in synergy, where accurate perception enables reliable prediction, and both are indispensable foundations for robust planning. However, conventional approaches with planning-only optimization neglect this interdependence, treating perception and prediction as byproducts rather than core components. Accordingly, we reconsider the role of GRPO in autonomous driving. Rather than restricting supervision to the planning stage alone, GRPO should be extended to explicitly encompass perception, prediction, and planning within a unified chain. Such a formulation ensures synergistic interactions across three modules and promotes coherent reasoning throughout the entire pipeline.

To address above fundamental limitations, we propose a novel three-module supervised GRPO algorithm specifically designed for the *AutoDrive-P<sup>3</sup>* framework, as illustrated in Fig. 1(d), which unifies Perception, Prediction, and Planning into a cohesive architecture. The *AutoDrive-P<sup>3</sup>* framework is capable of not only answering perception and prediction queries but also enhancing planning performance through synergistic interactions among all three modules. During the Supervised Fine-Tuning (SFT) stage, we train the model using our proposed *P<sup>3</sup>-CoT* dataset, resulting in the *AutoDrive-P<sup>3</sup>* base model. This model can generate responses following a structured perception-prediction-planning CoT format, thereby reducing the domain gap between VLMs and autonomous driving systems. Subsequently, inspired by the GRPO algorithm (Shao et al., 2024; Guo et al., 2025; Zhang et al., 2025), we propose *P<sup>3</sup>-GRPO* algorithm, which is a novel hierarchical and progressive optimization reinforcement fine-tuning (RFT) method that provides explicit supervision across perception, prediction, and planning modules. The *P<sup>3</sup>-GRPO* algorithm not only improves the accuracy of perception and prediction but also significantly enhances the model’s planning capability by ensuring coherent and context-aware decision-making.

We extensively evaluate *AutoDrive-P<sup>3</sup>* using real-world datasets, including the closed-loop **NAVSIMv1/v2** (Dauner et al., 2024; Cao et al., 2025) and the open-loop nuScenes (Caesar et al., 2020). Experimental results demonstrate that *AutoDrive-P<sup>3</sup>* achieves superior performance across various end-to-end autonomous driving benchmarks under both open-loop and closed-loop settings. More importantly, experimental results validate that our proposed *P<sup>3</sup>-GRPO* algorithm significantly enhances planning performance through its hierarchical and progressive supervision mechanism, which systematically improves perception and prediction capabilities and consequently leads to more reliable and accurate planning decisions. **Additionally, to balance inference efficiency with performance, we introduce dual thinking modes: detailed thinking and fast thinking.** The main contributions of this paper are summarized as follows:

1. We present *AutoDrive-P<sup>3</sup>*, an end-to-end vision-language driving framework that resolves a key limitation of current VLMs by explicitly capturing the relationship between perception, prediction, and planning in autonomous driving.
2. We introduce a three-module supervised *P<sup>3</sup>-GRPO* algorithm that provides hierarchical and progressive optimization across perception, prediction, and planning tasks, signifi-

108  
 109  
 110  
 111  
 112  
 113  
 114  
 115  
 116  
 117  
 118  
 119  
 120  
 121  
 122  
 123  
 124  
 125  
 126  
 127  
 128  
 129  
 130  
 131  
 132  
 133  
 134  
 135  
 136  
 137  
 138  
 139  
 140  
 141  
 142  
 143  
 144  
 145  
 146  
 147  
 148  
 149  
 150  
 151  
 152  
 153  
 154  
 155  
 156  
 157  
 158  
 159  
 160  
 161  
 cantly enhancing reasoning coherence and planning reliability by our proposed  $P^3\text{-}CoT$  dataset. Additionally, to balance efficiency with performance, we introduce dual thinking modes: detailed thinking and fast thinking.

3. We demonstrate that *AutoDrive-P<sup>3</sup>* achieves state-of-the-art performance on multiple autonomous driving benchmarks, including both open-loop and closed-loop tests, underscoring the effectiveness and generality of our approach.

## 2 RELATED WORK

### 2.1 END-TO-END AUTONOMOUS DRIVING METHODS

Autonomous driving systems have transitioned from traditional modular designs—featuring decoupled perception, prediction, and planning modules—toward end-to-end learning frameworks. Representative methods such as UniAD (Hu et al., 2023), ST-P3 (Hu et al., 2022) and VAD (Jiang et al., 2023) integrate these tasks into a single model trained jointly, improving planning performance. *DiffusionDrive* (Liao et al., 2025) integrates diffusion into trajectory planning, and *WoTE* (Li et al., 2025) leverages a BEV-based world model to predict future agent states, enabling online trajectory evaluation and selection. Though end-to-end autonomous driving methods make great progress, they still suffer from a lack of world knowledge and poor performance in long-tail scenarios.

### 2.2 VLM-BASED AUTONOMOUS DRIVING METHODS

Due to the limited capacity of such compact models and their constrained semantic understanding of complex environments, recent efforts increasingly incorporate Vision Language Models (VLMs) into driving systems. Approaches including DriveVLM (Tian et al., 2024), EMMA (Hwang et al., 2024), *VLM-AD* (Xu et al., 2024), OpenEMMA (Xing et al., 2025), OmniDrive (Wang et al., 2024), OpenDriveVLA (Zhou et al., 2025a), and AutoVLA (Zhou et al., 2025b) benefit from VLMs’ rich world knowledge and reasoning capabilities, demonstrating strong performance in driving scenarios. Nonetheless, while these methods are capable of answering QA-style queries about perception, prediction, and planning, they often address each task in a fragmented manner rather than through unified modeling. This lack of integration prevents the planning module from fully leveraging perceptual and predictive features, ultimately limiting overall planning performance.

### 2.3 GROUP RELATIVE POLICY OPTIMIZATION

The Group Relative Policy Optimization (GRPO) algorithm (Shao et al., 2024; Guo et al., 2025), introduced by DeepSeek, has demonstrated strong potential in enhancing the reasoning capabilities of Large Language Models (LLMs). With Vision-R1 (Huang et al., 2025) applying GRPO to Vision-Language Models (VLMs) and R1-VL (Zhang et al., 2025) further adopting step-wise reward mechanisms, GRPO has proven effective in improving VLM-based reasoning. In the context of autonomous driving, several works, such as AutoVLA (Zhou et al., 2025b), Plan-R1 (Tang et al., 2025), AlphaDrive (Jiang et al., 2025), and AutoDrive-R<sup>2</sup> (Yuan et al., 2025), have successfully incorporated GRPO to enhance the performance of driving-oriented VLMs. While these methods achieve notable results, they primarily rely on supervised learning only on the final planning outputs, without reinforcing perception and prediction modules through reward guidance. This narrow focus limits the synergistic effects between reasoning and low-level control, thus constraining the full potential of integrated planning capabilities.

## 3 PRELIMINARIES

**VLM-based End-to-end Autonomous Driving Problem Formulation.** We model end-to-end autonomous driving as mapping inputs to a trajectory  $Traj = \{(x_t, y_t)\}_{t=0}^T$ , where  $(x_t, y_t)$  is the ego vehicle’s position at time  $t$ . Given ego state  $E$ , sensor data  $S$ , and commands  $C$ , the trajectory distribution is autoregressively factorized as:

$$P(Traj | E, S, C) = \prod_{t=0}^T P((x_t, y_t) | E, S, C, (x_0, y_0), \dots, (x_{t-1}, y_{t-1})). \quad (1)$$

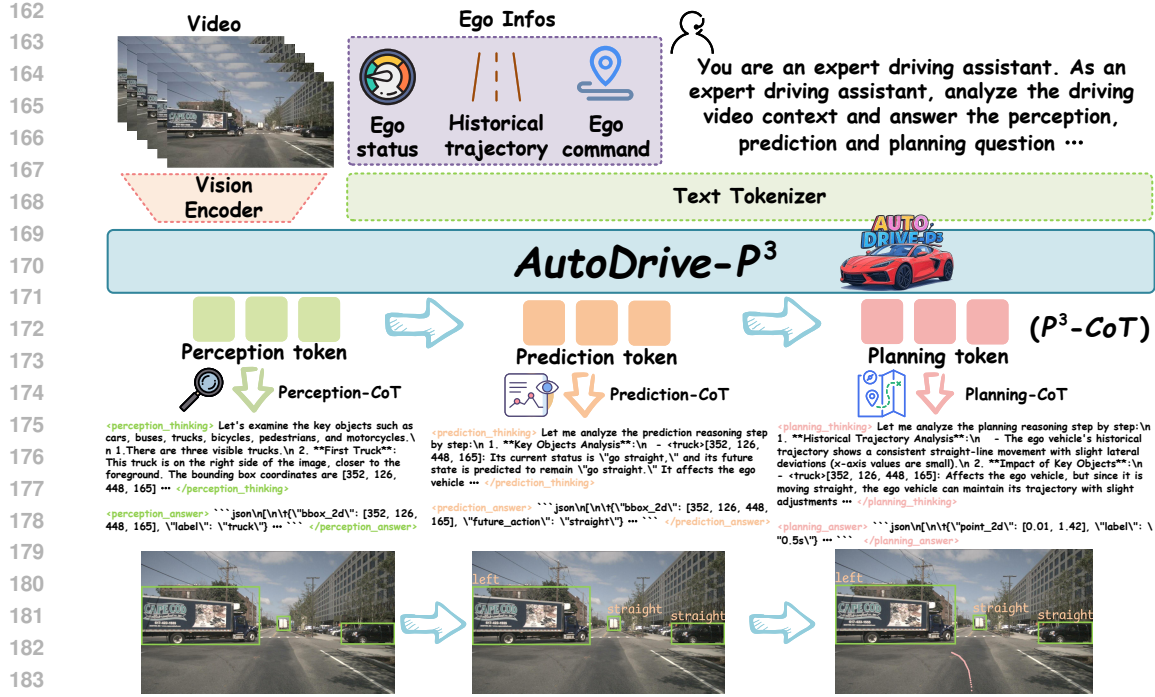


Figure 2: **Overview of AutoDrive-P<sup>3</sup>.** It processes video and ego vehicle data through structured Perception-Prediction-Planning Chain-of-Thought ( $P^3\text{-}CoT$ ) reasoning, generating interpretable step-by-step rationale and structured outputs for perception, prediction, and planning.

This formulation integrates all inputs to predict future positions sequentially, capturing temporal dependencies in a unified end-to-end framework.

**Group Relative Policy Optimization (GRPO).** GRPO improves learning stability by removing the dependence on a value function and optimizing a group-level, sample-wise objective (Shao et al., 2024). For each question-answer pair  $(q, a)$ , the behavior policy  $\pi_{\theta_{\text{old}}}$  generates a group of  $G$  responses  $\{o_i\}_{i=1}^G$ . The normalized advantage for the  $i$ -th response at step  $t$  is computed as:

$$\hat{A}_{i,t} = \frac{R_i - \text{mean}(\{R_j\}_{j=1}^G)}{\text{std}(\{R_j\}_{j=1}^G)}, \quad (2)$$

where  $R_i$  is the reward of the  $i$ -th response. The GRPO objective integrates a clipped surrogate loss with a KL penalty term:

$$\mathcal{J}_{\text{GRPO}}(\theta) = \mathbb{E}_{q, \{o_i\} \sim \pi_{\theta_{\text{old}}}(O|q)} \left[ \frac{1}{G} \sum_{i=1}^G \left( \mathcal{J}_i^R - \beta D_{\text{KL}}(\pi_{\theta} \| \pi_{\text{ref}}) \right) \right], \quad (3)$$

$$\mathcal{J}_i^R = \min \left( \frac{\pi_{\theta}(o_i|q)}{\pi_{\theta_{\text{old}}}(o_i|q)} A_i, \text{clip} \left( \frac{\pi_{\theta}(o_i|q)}{\pi_{\theta_{\text{old}}}(o_i|q)}, 1 - \epsilon, 1 + \epsilon \right) A_i \right). \quad (4)$$

By leveraging diverse responses sampled from the model itself, GRPO enhances the model's reasoning capability through exposure to varied reasoning paths and solutions.

## 4 METHODOLOGY

In this section, we propose the *AutoDrive-P<sup>3</sup>* framework, which integrates Perception, Prediction, and Planning for autonomous driving. Existing VLM-based datasets offer only fragmented QA pairs, unsuitable for GRPO training. To solve this, we create the  $P^3\text{-}CoT$  dataset with unified CoT sequences linking the three tasks. We then perform supervised fine-tuning for cold-start initialization to align VLMs with the autonomous driving domain and generate accurate  $P^3\text{-}CoT$  outputs. Finally, the  $P^3\text{-}GRPO$  algorithm is introduced for post-training, providing hierarchical supervision and enabling collaborative optimization across modules to improve planning via iterative CoT reasoning.

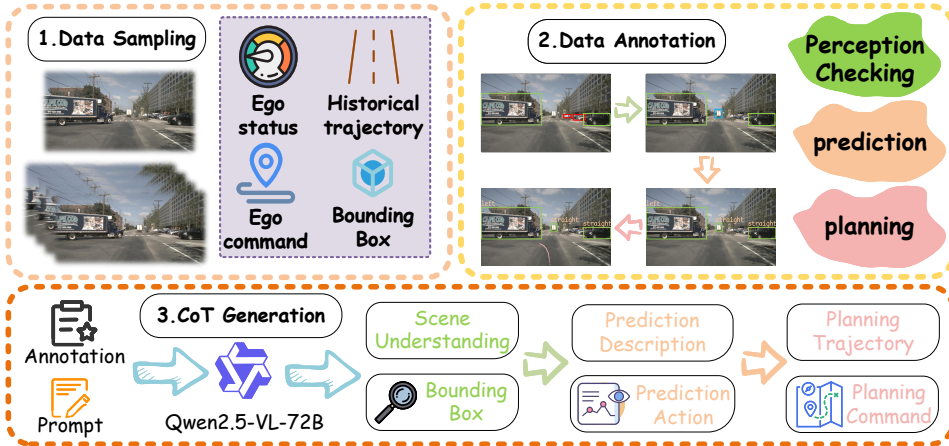


Figure 3: **The pipeline for constructing  $P^3$ -CoT dataset.** We first sample data and annotations from existing datasets, then construct the labels of samples, focusing on key objects and using rule-based and manual filtering. Finally, with the help of advanced VLM, we construct the CoT, focusing on the connection among perception, prediction and planning three stages.

#### 4.1 $P^3$ -CoT DATASET

To cover all the thinking steps of human drivers and meet the need of VLMs, a high quality reasoning dataset with key objects and detailed CoT annotations is strongly recommended. However, the following key challenges remain to be addressed: 1) lack of completed and comprehensive key object annotations, 2) requirements of unified chain of thought datasets for perception, prediction and planning, 3) a proper CoT format suitable for VLM training instead of question-and-answer pairs. To address these issues, we propose  $P^3$ -CoT dataset, a high-quality key objects’ labels with CoT designed for VLM GRPO post-training, as shown in Fig. 3. We first identify and annotate critical objects in each key frame of the original dataset based on their potential impact on vehicle navigation, marking their bounding boxes as perception labels. We then derive prediction labels by projecting these critical objects’ future trajectories. Finally, planning labels are obtained from the ego vehicle’s planned trajectory. With these three-stage labels, we employ Qwen2.5-VL-72B (Bai et al., 2025) to generate coherent CoT data that seamlessly connects all three stages, with manual verification to ensure the correctness and logical integrity of the synthesized reasoning chains. Employing this annotation pipeline, we organize a high-quality and comprehensive CoT dataset with key object annotation and a unified  $P^3$  architecture in CoT format.  $P^3$ -CoT includes 25303 frames from 850 scenes based on nuScenes, and 115434 frames from 1382 scenes based on NAVSIM. Additional description, statistics, and examples are attached in Appendix B.

Furthermore, we highlight that the proposed  $P^3$ -CoT dataset benefits the model at both the holistic and modular levels. From a holistic perspective, the sequential reasoning process—from perception to prediction, and then to planning—guides the model in developing coherent and strategic driving behaviors. At the modular level, the specialized CoTs for perception, prediction, and planning respectively enhance the model’s accuracy and reliability in executing each subtask. Comprehensive experiments in Section 5 validate these benefits across both levels.

#### 4.2 SUPERVISED FINE-TUNING FOR COLD-START

To equip a VLM with autonomous-driving knowledge and structured reasoning capabilities, we conduct supervised fine-tuning (SFT) using the proposed  $P^3$ -CoT dataset. As illustrated in Fig. 2, the model processes multimodal inputs  $x = [x_{\text{ego}}; x_{\text{video}}; x_{\text{cmd}}; x_{\text{prompt}}]$  and learns to generate structured outputs organized into perception, prediction, and planning modules. The target output follows a unified format for each module:

$$y = [y_{\text{perception}}; y_{\text{prediction}}; y_{\text{planning}}], \quad \text{where} \quad y_{\text{module}} = [y_{\text{thinking}}; y_{\text{answer}}]. \quad (5)$$

This approach enables the model to produce coherent reasoning traces followed by concrete answers, establishing a foundational capability for Chain-of-Thought reasoning across all three autonomous



Figure 4: **The pipeline of  $P^3$ -GRPO.** We first cold start the base model using  $P^3$ -CoT to make up for the gap between VLM and autonomous driving and learn the CoT answer format. Next we use GRPO to find the best optimization path and update our model.

driving stages. The training objective minimizes the negative log-likelihood of the target sequence:

$$\mathcal{L}_{\text{SFT}} = - \sum_{t=1}^T \log P(y_t \mid y_{t-1}, x), \quad (6)$$

where  $T$  is the total length of the target sequence. After cold-start SFT, the VLM acquires essential driving capabilities and produces interpretable  $P^3$ -CoT outputs that enhance both transparency and performance, forming a solid basis for subsequent reinforcement learning.

### 4.3 $P^3$ -GRPO ALGORITHM

Following the cold-start SFT phase, we further enhance the VLM’s reasoning capability across all three stages by applying the GRPO algorithm to the perception, prediction, and planning modules collectively, yielding the  $P^3$ -GRPO algorithm, as shown in Fig. 4. Our approach employs a multi-component reward function to guide the policy model toward generating accurate, coherent, and well-structured outputs through coordinated reinforcement learning across these cognitive layers. The overall reward is computed as a weighted sum of the following components:

$$R(q, a) = \lambda_{\text{format}} \cdot R_{\text{format}} + \lambda_{\text{perc}} \cdot R_{\text{perc}} + \lambda_{\text{pred}} \cdot R_{\text{pred}} + \lambda_{\text{plan}} \cdot R_{\text{plan}}, \quad (7)$$

where  $\lambda_{\text{format}}$ ,  $\lambda_{\text{perc}}$ ,  $\lambda_{\text{pred}}$ , and  $\lambda_{\text{plan}}$  are weighting coefficients for each reward term. This integrated reward structure explicitly encodes the causal relationship between modules: perception enables prediction, and together they provide the necessary foundation for effective planning. By simultaneously optimizing together, our approach ensures that improvements in planning accuracy are grounded in corresponding enhancements in perceptual understanding and predictive capability.

**Perception Reward ( $R_{\text{perc}}$ )** measures object detection quality based on average IoU, precision ( $P$ ), and recall ( $R$ ), which encourages accurate and spatially precise perception, enabling reliable prediction and planning reasoning:

$$R_{\text{perc}} = \begin{cases} 1.0, & \text{if } |\mathcal{B}_{\text{gt}}| = 0 \text{ and } |\mathcal{B}_{\text{pred}}| = 0, \\ \text{IoU}_{\text{avg}} \cdot (0.5P + 0.5R), & \text{if } |\mathcal{B}_{\text{gt}}| > 0 \text{ and } |\mathcal{B}_{\text{pred}}| > 0, \\ 0.0, & \text{otherwise.} \end{cases} \quad (8)$$

**Prediction Reward ( $R_{\text{pred}}$ )** evaluates forecasting accuracy by combining behavior label correctness weighted by IoU and detection quality, which links perceptual accuracy with semantic correctness to foster robust prediction:

$$R_{\text{pred}} = \left( \frac{\sum_{(i,j) \in \mathcal{M}} \text{IoU}_{ij} \cdot \mathbb{I}(s_i = s_j)}{\sum_{(i,j) \in \mathcal{M}} \text{IoU}_{ij}} \right) \times (\text{IoU}_{\text{avg}} \cdot (0.5P + 0.5R)). \quad (9)$$

**Planning Reward ( $R_{\text{plan}}$ )** quantifies trajectory quality via L2 distance:

$$R_{\text{plan}} = \frac{2}{1 + e^{\text{clip}(L2, 0, L2_{\text{max}})}}. \quad (10)$$

---

**Algorithm 1**  $P^3$ -GRPO: Perception-Prediction-Planning Group Relative Policy Optimization
 

---

324  
 325  
 326 **Require:** Policy model  $\pi_\theta$  with  $P^3$ -CoT; dataset  $\mathcal{D} = \{Q_n\}_{n=1}^N$ ; reward weights  $\lambda_{\text{format}}, \lambda_{\text{perc}},$   
 327  $\lambda_{\text{pred}}, \lambda_{\text{plan}}$ ; KL constraint  $\beta$ ; clip param  $\epsilon$ .  
 328 **Ensure:** Optimized policy model  $\pi_\theta$   
 329 1: **for** iter = 1 to  $N_{\text{RL}}$  **do**  
 330 2: Sample query  $Q \sim \mathcal{D}$   
 331 3: Generate group of responses  $\{a_i\}_{i=1}^M \sim \pi_\theta(\cdot|Q)$   
 332 4: **for**  $i = 1$  to  $M$  **do**  
 333 5: Parse  $a_i$  into perception, prediction, planning components  
 334 6: Compute rewards:  $R_{\text{format}}^i, R_{\text{perc}}^i, R_{\text{pred}}^i, R_{\text{plan}}^i$   
 335 7: Aggregate reward:  $R_i = \lambda_{\text{format}} R_{\text{format}}^i + \lambda_{\text{perc}} R_{\text{perc}}^i + \lambda_{\text{pred}} R_{\text{pred}}^i + \lambda_{\text{plan}} R_{\text{plan}}^i$   
 336 8: **end for**  
 337 9: Compute mean  $\bar{R} = \frac{1}{M} \sum_i R_i$  and std  $\sigma_R = \sqrt{\frac{1}{M} \sum_i (R_i - \bar{R})^2}$   
 338 10: **for**  $i = 1$  to  $M$  **do**  
 339 11: Normalize advantage:  $A_i = \frac{R_i - \bar{R}}{\sigma_R}$   
 340 12: **end for**  
 341 13: **for**  $i = 1$  to  $M$  **do**  
 342 14: Compute ratio  $r_i = \frac{\pi_\theta(a_i|Q)}{\pi_{\text{old}}(a_i|Q)}$   
 343 15: Surrogate objective:  $J_i = \min(r_i A_i, \text{clip}(r_i, 1 - \epsilon, 1 + \epsilon) A_i)$   
 344 16: **end for**  
 345 17: Compute policy loss:  $\mathcal{L}_{\text{policy}} = -\frac{1}{M} \sum_i J_i$ , KL penalty:  $\mathcal{L}_{\text{KL}} = \beta D_{\text{KL}}(\pi_\theta || \pi_{\text{ref}})$   
 346 18: Update  $\pi_\theta$  via gradient descent on  $\mathcal{L}_{\text{policy}} + \mathcal{L}_{\text{KL}}$   
 347 19: **end for**  
 348 20: **return**  $\pi_\theta$ 


---

Table 1: Performance comparison on nuScenes Benchmark.

Method	L2 (m) ↓				Collision (%) ↓				VLM
	1s	2s	3s	Avg.	1s	2s	3s	Avg.	
Non-Autoregressive Methods									
ST-P3 (Hu et al., 2022)	1.33	2.11	2.90	2.11	0.23	0.62	1.27	0.71	-
VAD (Jiang et al., 2023)	0.17	0.34	0.60	0.37	0.07	0.10	0.24	0.14	-
Ego-MLP (Li et al., 2024d)	0.46	0.76	1.12	0.78	0.21	0.35	0.58	0.38	-
UniAD (Hu et al., 2023)	0.44	0.67	0.96	0.69	0.04	0.08	0.23	0.12	-
InsightDrive (Song et al., 2025)	0.23	0.41	0.68	0.44	0.09	0.10	0.27	0.15	-
Autoregressive Methods									
GPT-Driver (Mao et al., 2023)	0.20	0.40	0.70	0.44	0.04	0.12	0.36	0.17	GPT-3.5
DriveVLM (Tian et al., 2024)	0.18	0.34	0.68	0.40	0.10	0.22	0.45	0.27	Qwen2-VL-7B
OpenEMMA (Xing et al., 2025)	1.45	3.21	3.76	2.81	-	-	-	-	Qwen2-VL-7B
RDA-Driver (Huang et al., 2024a)	0.17	0.37	0.69	0.40	0.01	0.05	0.26	0.10	LLaVa-7B
OmniDrive (Wang et al., 2024)	<b>0.14</b>	<b>0.29</b>	<b>0.55</b>	<b>0.33</b>	<b>0.01</b>	<b>0.04</b>	<b>0.27</b>	<b>0.11</b>	LLava-7B
OpenDriveVLA (Zhou et al., 2025a)	<b>0.14</b>	<b>0.30</b>	<b>0.55</b>	<b>0.33</b>	<b>0.02</b>	<b>0.07</b>	<b>0.22</b>	<b>0.10</b>	Qwen2.5-VL-3B
AutoVLA (Zhou et al., 2025b)	0.25	0.46	0.73	0.48	0.07	0.07	0.26	0.13	Qwen2.5-VL-3B
AutoDrive-R <sup>2</sup> (Yuan et al., 2025)	0.35	0.49	0.62	0.49	-	-	-	-	Qwen2.5-VL-3B
<i>AutoDrive-P<sup>3</sup></i> (Ours-Detailed)	<b>0.15</b>	<b>0.30</b>	<b>0.54</b>	<b>0.33</b>	<b>0.00</b>	<b>0.02</b>	<b>0.15</b>	<b>0.06</b>	Qwen2.5-VL-3B
<i>AutoDrive-P<sup>3</sup></i> (Ours-Fast)	<b>0.16</b>	<b>0.31</b>	<b>0.56</b>	<b>0.34</b>	<b>0.00</b>	<b>0.04</b>	<b>0.20</b>	<b>0.08</b>	Qwen2.5-VL-3B

364  
 365 These rewards together form a coordinated learning signal that promotes synergy among perception,  
 366 prediction, and planning, ultimately driving accurate and interpretable autonomous driving behavior.  
 367 The complete algorithmic procedure is summarized in Algorithm 1. Detailed formulations and  
 368 comprehensive analyses of each reward component are provided in the Appendix C.

## 5 EXPERIMENTS

### 5.1 BENCHMARKS

372 **nuScenes** (Caesar et al., 2020). The nuScenes dataset comprises 1,000 real-world driving sequences.  
 373 Following established evaluation protocols in related works (Hu et al., 2023; Jiang et al., 2023;  
 374 Wang et al., 2024; Zhou et al., 2025a), we adopt two key metrics for planning performance: L2  
 375 displacement error and collision rate, using the same ST-P3 (Hu et al., 2022) metric settings.

377 **NAVSIM** (Dauner et al., 2024; Cao et al., 2025). To address the limited complexity of nuScenes,  
 378 we further validate our approach using the NAVSIM benchmark. **NAVSIMv1** (Dauner et al., 2024)

378  
379  
380 Table 2: Performance comparison on NAVSIMv1 benchmark.  
381  
382  
383  
384  
385  
386  
387  
388  
389  
390  
391  
392  
393  
394

Method	Image	Lidar	NC↑	DAC↑	EP↑	TTC↑	Comf↑	PDMS↑
Human	✗	✗	100.0	100.0	87.5	100.0	99.9	94.8
Constant Velocity	✗	✗	69.9	58.8	49.3	49.3	100.0	21.6
Ego Status MLP	✗	✗	93.0	77.3	62.8	83.6	100.0	65.6
VADv2 (Weng et al., 2024)	✓	✗	97.9	91.7	77.6	92.9	100.0	83.0
UniAD (Hu et al., 2023)	✓	✗	97.8	91.9	78.8	92.9	100.0	83.4
LTf (Prakash et al., 2021)	✓	✗	97.4	92.8	79.0	92.4	100.0	83.8
TransFuser (Prakash et al., 2021)	✓	✓	97.7	92.8	79.2	92.8	100.0	84.0
PARA-Drive (Weng et al., 2024)	✓	✗	97.9	92.4	79.3	93.0	99.8	84.0
LAW (Li et al., 2024a)	✓	✓	96.4	95.4	81.7	88.7	99.9	84.6
DRAMA (Yuan et al., 2024)	✓	✓	98.0	93.1	80.1	94.8	100.0	85.5
Hydra-MDP (Li et al., 2024b)	✓	✓	98.3	96.0	78.7	94.6	100.0	86.5
DiffusionDrive (Liao et al., 2025)	✓	✓	98.2	96.2	82.2	94.7	100.0	88.1
WoTE (Li et al., 2025)	✓	✓	98.5	96.8	81.9	94.9	99.9	88.3
<i>AutoDrive-P<sup>3</sup></i> (Ours-Detailed)	✓	✗	99.1	97.4	84.8	96.5	100.0	90.6
<i>AutoDrive-P<sup>3</sup></i> (Ours-Fast)	✓	✗	98.9	97.7	83.7	96.6	99.9	90.2

395 employs a simulation environment and uses the Predictive Driver Model Score (PDMS) for closed-  
396 loop evaluation. The PDMS is a composite metric defined as:

$$397 \quad \text{PDMS} = \text{NC} \times \text{DAC} \times \left( \frac{5 \times \text{EP} + 5 \times \text{TTC} + 2 \times \text{Comf}}{12} \right), \quad (11)$$

400 where the components include No Collision (NC), Drivable Area Compliance (DAC), Ego Progress  
401 (EP), Time-to-Collision (TTC), and Comfort (Comf). In addition, NAVSIMv2 (Cao et al., 2025)  
402 offers a more comprehensive metric, named Extended Predictive Driver Model Score (EPDMS):  
403

$$404 \quad \text{EPDMS} = \text{NC} \times \text{DAC} \times \text{DDC} \times \text{TLC} \times \left( \frac{5 \times \text{EP} + 5 \times \text{TTC} + 2 \times \text{LK} + 2 \times \text{HC} + 2 \times \text{EC}}{12} \right), \quad (12)$$

407 where the components include Driving Direction Compliance (DDC), Traffic Light Compliance  
408 (TLC), Lane Keeping (LK), History Comfort (HC), Extended Comfort (EC) and other metrics are  
409 the same as PDMS. To reduce false positive penalties, NAVSIMv2 sets “human\_penalty\_filter” to  
410 true, disabling penalties when the human agent makes a violation; otherwise, it is set to false.

411  
412 Table 3: Performance comparison on NAVSIMv2 benchmark.

Method	NC↑	DAC↑	DDC↑	TLC↑	EP↑	TTC↑	LK↑	HC↑	EC↑	EPDMS↑ False / True
Human	100.0	100.0	99.8	100.0	87.4	100.0	100.0	98.1	90.1	90.3 / 94.5
Ego Status MLP	93.1	77.9	92.7	99.6	86.0	91.5	89.4	98.3	85.4	64.0 / -
Transfuser (Prakash et al., 2021)	96.9	89.9	97.8	99.7	87.1	95.4	92.7	98.3	87.2	76.7 / 84.0
HydraMDP++ (Li et al., 2024b)	97.2	97.5	99.4	99.6	83.1	96.5	94.4	98.2	70.9	81.4 / -
DiffusionDrive (Liao et al., 2025)	98.2	96.2	99.5	99.8	87.4	97.3	96.9	98.4	87.7	84.7 / 88.2
WoTE (Li et al., 2025)	98.5	96.8	98.8	99.8	86.1	97.9	95.5	98.3	82.9	84.2 / 87.7
<i>AutoDrive-P<sup>3</sup></i> (Ours-Detailed)	99.1	97.4	99.2	99.8	88.0	98.7	96.3	98.3	85.5	86.2 / 89.9
<i>AutoDrive-P<sup>3</sup></i> (Ours-Fast)	98.9	97.6	98.9	99.8	86.8	98.5	95.4	98.3	80.6	85.2 / 88.7

421  
422 5.2 IMPLEMENTATION DETAILS

423  
424 **nuScenes Benchmark.** Model inputs consist of 3-second video clips composed of 6 frames, drawn  
425 solely from the front-view camera. Images are resized to a resolution of 448×252. The ego-state  
426 information provided is only ego speed. The model is trained for 10 epochs with a batch size of 8.

427  
428 **NAVSIM Benchmark.** Model input is constructed from 2-second video segments containing 4  
429 frames, combining the front, front-left, and front-right camera views, which is then resized to  
430 672×168. The ego-state information includes the longitudinal and lateral velocity and acceleration  
431 components (i.e.,  $v_x, v_y, a_x, a_y$ ). The model is trained for 10 epochs with a batch size of 32.

432  
433 **Shared Settings.** We use Qwen2.5-VL-3B (Bai et al., 2025) as base model. All models are op-  
434 timized using the AdamW optimizer across 8 A100 GPUs. During training with  $P^3$ -GRPO, 8

432  
433  
434 Table 4: **Ablation study on AutoDrive- $P^3$  on nuScenes Benchmark.**  
435  
436  
437  
438  
439  
440

Method	Perception $\uparrow$	Prediction $\uparrow$	Planning (Collision, %) $\downarrow$			
			1s	2s	3s	Avg.
UniAD (Hu et al., 2023)	0.32	0.31	0.04	0.08	0.23	0.12
OmniDrive (Wang et al., 2024)	0.37	–	0.01	0.04	0.27	0.11
<i>AutoDrive-<math>P^3</math></i> (Only SFT)	0.33	0.23	0.01	0.08	0.40	0.17
<i>AutoDrive-<math>P^3</math></i> (SFT + Only Planning GRPO)	–	–	0.03	0.08	0.24	0.12
<i>AutoDrive-<math>P^3</math></i> (SFT + $P^3$ -GRPO)	<b>0.64</b>	<b>0.54</b>	<b>0.00</b>	<b>0.02</b>	<b>0.15</b>	<b>0.06</b>

441  
442 Table 5: **Ablation study on different training setting on nuScenes benchmark.**  
443  
444

Method	Group Size	History Traj.	Sensor Type	L2 (m) $\downarrow$				Collision (%) $\downarrow$			
				1s	2s	3s	Avg.	1s	2s	3s	Avg.
Ablation 1	4	✓	Video	0.17	0.32	0.65	0.38	0.01	0.06	0.30	0.13
Ablation 2	8	✗	Video	0.17	0.33	0.68	0.39	0.02	0.07	0.33	0.14
Ablation 3	8	✓	Image	0.16	0.32	0.61	0.36	0.01	0.05	0.26	0.12
$P^3$ -GRPO	8	✓	Video	<b>0.15</b>	<b>0.30</b>	<b>0.54</b>	<b>0.33</b>	<b>0.00</b>	<b>0.02</b>	<b>0.15</b>	<b>0.06</b>

450  $P^3$ -CoT samples are generated for each scenario. The reward function incorporates multiple components balanced by the following weights:  $\lambda_{\text{format}}$ ,  $\lambda_{\text{perc}}$ ,  $\lambda_{\text{pred}}$ , and  $\lambda_{\text{plan}}$  in a ratio of 1:2:2:5. Following (Zhou et al., 2025b), we add PDMS to planning reward for NAVSIM benchmark. For each benchmark, we implement a dual-thinking setup consisting of a fast and a detailed version, as shown in Fig. 5. The fast version is designed for efficiency; while it adheres to the  $P^3$ -CoT structure, it only yields the final answer from each module without reasoning. The detailed version, in contrast, provides the complete reasoning with answer for all modules.

### 458 5.3 COMPARISON WITH STATE-OF-THE-ART METHODS

460 As show in Table 1, we compare *AutoDrive- $P^3$*  with mainstream methods on nuScenes dataset. We  
461 achieve the same level as SOTA methods at L2 and overpass about 40% compared to SOTA methods  
462 at collision rare. In Table 2 and Table 3, *AutoDrive- $P^3$*  achieves the SOTA results with vision-  
463 only input on NAVSIMv1/v2 benchmark, achieving 90.6 PDMS and 89.9 EPDMS. Specifically, our  
464 method achieves comparable L2 scores with a significantly smaller model (Qwen2.5-3B vs. LLava-  
465 7B used in OmniDrive) and less training data (20k vs. 1000k samples used in OpenDriveVLA),  
466 while also attaining the best collision rate, demonstrating the superior efficiency and effectiveness  
467 of *AutoDrive- $P^3$* .

### 468 5.4 ABLATION STUDY

469 **Ablation Study on *AutoDrive- $P^3$* .** We conduct ablation studies on *AutoDrive- $P^3$*  with nuScenes  
470 to assess the effectiveness of joint RFT across perception–prediction–planning. We compare three  
471 settings—(1) Only SFT, (2) SFT + Only Planning GRPO, and (3) SFT +  $P^3$ -GRPO—against two  
472 end-to-end baselines: the small-scale UniAD and the VLM-based OmniDrive. As shown in Ta-  
473 ble 4, Only SFT already achieves a lower 2s collision rate than baselines. Adding Planning GRPO  
474 further reduces the 3s collision rate, matching baseline performance. Crucially,  $P^3$ -GRPO yields  
475 large improvements in perception and prediction, surpassing all baselines and significantly boost-  
476 ing planning. These results demonstrate that  $P^3$ -GRPO effectively captures the staged CoT across  
477 perception, prediction, and planning, leading to holistic gains in autonomous driving.

478 **Ablation Study on Training Settings.** We conduct additional ablation studies on three training  
479 configurations: GRPO group size, historical trajectory usage, and sensor modality. As shown in Ta-  
480 ble 5, results demonstrate that: (1) increasing group size from 4 to 8 enhances performance through  
481 more diverse reasoning samples; (2) incorporating historical trajectories improves contextual un-  
482 derstanding; and (3) video sensors outperform image-based inputs by capturing temporal dynamics.  
483 Our full configuration achieves optimal results across all metrics.

484 **Runtime and Dual thinking modes.** We provide dual thinking modes’ inference time compared  
485 to other methods, as shown in Fig. 5. We employ FlashAttention-2 (Dao, 2023) and vLLM 0.8.0  
(Kwon et al., 2023) acceleration on an A100 GPU, achieving near real-time performance (1 Hz).

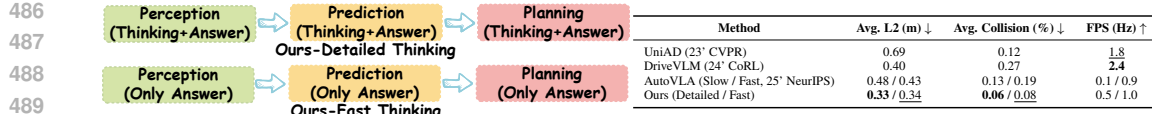


Figure 5: Dual thinking modes and running time on nuScenes Benchmark.

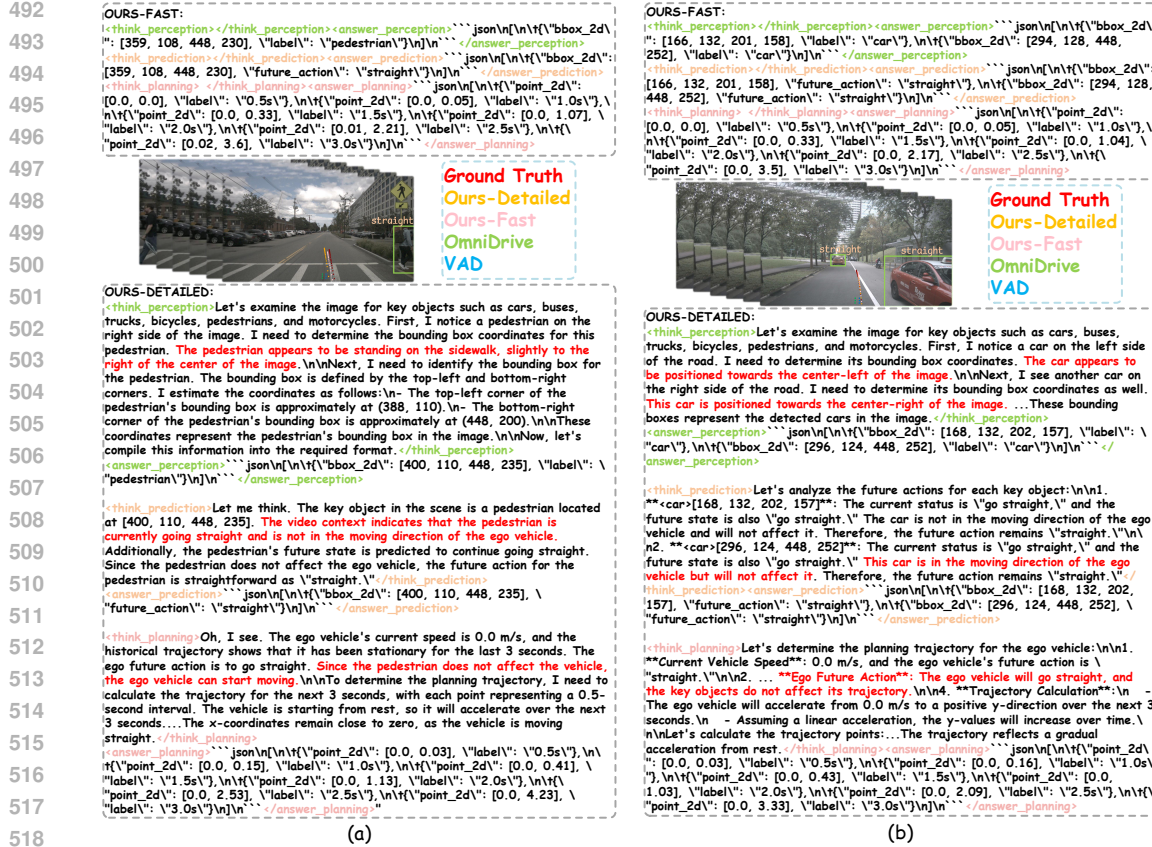


Figure 6: Visualization. Our model, taking into account the scenarios comprehensively, makes efficient plans that are both reasonable and safe.

## 5.5 VISUALIZATION

Fig. 6(a) demonstrates our method's ability to accurately perceive pedestrian location and predict safe passage opportunities, avoiding the overly conservative decisions of comparison methods. In Fig. 6(b), our approach successfully handles complex vehicle interactions by identifying key objects and their behaviors, producing trajectories that align with human driving habits.

## 6 CONCLUSION AND FUTURE WORK

In this work, we proposed *AutoDrive-P<sup>3</sup>*, a novel VLM framework that establishes progressive connections between Perception, Prediction, and Planning. Our approach includes the *P<sup>3</sup>-CoT* dataset with unified reasoning chains and labels, supervised fine-tuning for domain adaptation, and the *P<sup>3</sup>-GRPO* algorithm for hierarchical multi-task supervision. Experiments on **NAVSIMv1/v2** and nuScenes show state-of-the-art performance, reducing collision rate by 40% on nuScenes. To balance inference efficiency with performance, we introduce dual thinking modes: detailed thinking and fast thinking. Although *AutoDrive-P<sup>3</sup>* achieves state-of-the-art performance, it faces limitations in hallucinatory phenomena during reasoning. Additionally, our reinforcement learning is conducted in offline simulators, lacking interaction with real-world environments. Future work will focus on mitigating hallucinations, reducing inference time, and deploying the system in closed-loop settings.

540      **7 ETHICS STATEMENT**

541

542      This work adheres to the ICLR Code of Ethics and all authors have read and adhered to the Code  
 543      of Ethics. In this study, no human subjects is involved. The use of all datasets, including nuScenes  
 544      (Caesar et al., 2020) and NAVSIM (Dauner et al., 2024; Cao et al., 2025), follows the relevant usage  
 545      guidelines and public licenses, ensuring no violation of privacy. We have been careful to avoid any  
 546      biased or discriminatory results during our research process. No personally identifiable information  
 547      is used, and no privacy or security concerns will be raised due to our experiments. We are committed  
 548      to maintaining transparency and integrity throughout the research process.

549

550      **8 REPRODUCIBILITY STATEMENT**

551

552      We have made every effort to ensure that the results presented in this paper are reproducible. All  
 553      code and datasets have been made publicly available in an anonymous repository to facilitate repli-  
 554      cation and verification. The experimental setup, including training steps, model configurations, and  
 555      hardware details, is described in detail in the paper. We have also provided a full description of  
 556      *AutoDrive-P<sup>3</sup>* to assist others in reproducing our experiments.

557      Additionally, the datasets used in our experiments are publicly available, ensuring consistent and  
 558      reproducible evaluation results.

559      We believe these measures will enable other researchers to reproduce our work and further advance  
 560      the field.

561

562      **REFERENCES**

563

564      Shuai Bai, Keqin Chen, Xuejing Liu, Jialin Wang, Wenbin Ge, Sibo Song, Kai Dang, Peng Wang,  
 565      Shijie Wang, Jun Tang, et al. Qwen2. 5-vl technical report. *arXiv preprint arXiv:2502.13923*,  
 566      2025.

567      Holger Caesar, Varun Bankiti, Alex H Lang, Sourabh Vora, Venice Erin Liong, Qiang Xu, Anush  
 568      Krishnan, Yu Pan, Giancarlo Baldan, and Oscar Beijbom. nuscenes: A multimodal dataset for  
 569      autonomous driving. In *Proceedings of the IEEE/CVF conference on computer vision and pattern*  
 570      *recognition*, pp. 11621–11631, 2020.

571

572      Wei Cao, Marcel Hallgarten, Tianyu Li, Daniel Dauner, Xunjiang Gu, Caojun Wang, Yakov Miron,  
 573      Marco Aiello, Hongyang Li, Igor Gilitschenski, et al. Pseudo-simulation for autonomous driving.  
 574      *arXiv preprint arXiv:2506.04218*, 2025.

575      Tri Dao. Flashattention-2: Faster attention with better parallelism and work partitioning. *arXiv*  
 576      *preprint arXiv:2307.08691*, 2023.

577      Daniel Dauner, Marcel Hallgarten, Tianyu Li, Xinshuo Weng, Zhiyu Huang, Zetong Yang,  
 578      Hongyang Li, Igor Gilitschenski, Boris Ivanovic, Marco Pavone, et al. Navsim: Data-driven  
 579      non-reactive autonomous vehicle simulation and benchmarking. *Advances in Neural Information*  
 580      *Processing Systems*, 37:28706–28719, 2024.

581

582      Xinpeng Ding, Jianhua Han, Hang Xu, Xiaodan Liang, Wei Zhang, and Xiaomeng Li. Holistic au-  
 583      tonomous driving understanding by bird’s-eye-view injected multi-modal large models. In *Pro-  
 584      ceedings of the IEEE/CVF Conference on Computer Vision and Pattern Recognition*, pp. 13668–  
 585      13677, 2024.

586

587      Daya Guo, Dejian Yang, Haowei Zhang, Junxiao Song, Ruoyu Zhang, Runxin Xu, Qihao Zhu,  
 588      Shirong Ma, Peiyi Wang, Xiao Bi, et al. Deepseek-r1: Incentivizing reasoning capability in llms  
 589      via reinforcement learning. *arXiv preprint arXiv:2501.12948*, 2025.

590

591      Shengchao Hu, Li Chen, Penghao Wu, Hongyang Li, Junchi Yan, and Dacheng Tao. St-p3: End-to-  
 592      end vision-based autonomous driving via spatial-temporal feature learning. In *European Confer-  
 593      ence on Computer Vision*, pp. 533–549. Springer, 2022.

594 Yihan Hu, Jiazhi Yang, Li Chen, Keyu Li, Chonghao Sima, Xizhou Zhu, Siqi Chai, Senyao Du,  
 595 Tianwei Lin, Wenhai Wang, et al. Planning-oriented autonomous driving. In *Proceedings of the*  
 596 *IEEE/CVF conference on computer vision and pattern recognition*, pp. 17853–17862, 2023.

597

598 Wenzuan Huang, Bohan Jia, Zijie Zhai, Shaosheng Cao, Zheyu Ye, Fei Zhao, Zhe Xu, Yao Hu, and  
 599 Shaohui Lin. Vision-r1: Incentivizing reasoning capability in multimodal large language models.  
 600 *arXiv preprint arXiv:2503.06749*, 2025.

601

602 Zhijian Huang, Tao Tang, Shaoxiang Chen, Sihao Lin, Zequn Jie, Lin Ma, Guangrun Wang, and Xi-  
 603 aodan Liang. Making large language models better planners with reasoning-decision alignment.  
 604 In *European Conference on Computer Vision*, pp. 73–90. Springer, 2024a.

605

606 Zhiyu Huang, Xinshuo Weng, Maximilian Igl, Yuxiao Chen, Yulong Cao, Boris Ivanovic, Marco  
 607 Pavone, and Chen Lv. Gen-drive: Enhancing diffusion generative driving policies with reward  
 608 modeling and reinforcement learning fine-tuning. *arXiv preprint arXiv:2410.05582*, 2024b.

609

610 Jyh-Jing Hwang, Runsheng Xu, Hubert Lin, Wei-Chih Hung, Jingwei Ji, Kristy Choi, Di Huang,  
 611 Tong He, Paul Covington, Benjamin Sapp, et al. Emma: End-to-end multimodal model for au-  
 612 tonomous driving. *arXiv preprint arXiv:2410.23262*, 2024.

613

614 Bo Jiang, Shaoyu Chen, Qing Xu, Bencheng Liao, Jiajie Chen, Helong Zhou, Qian Zhang, Wenyu  
 615 Liu, Chang Huang, and Xinggang Wang. Vad: Vectorized scene representation for efficient au-  
 616 tonomous driving. In *Proceedings of the IEEE/CVF International Conference on Computer Vi-  
 617 sion*, pp. 8340–8350, 2023.

618

619 Bo Jiang, Shaoyu Chen, Qian Zhang, Wenyu Liu, and Xinggang Wang. Alphadrive: Unleashing the  
 620 power of vlms in autonomous driving via reinforcement learning and reasoning. *arXiv preprint*  
 621 *arXiv:2503.07608*, 2025.

622

623 Woosuk Kwon, Zhuohan Li, Siyuan Zhuang, Ying Sheng, Lianmin Zheng, Cody Hao Yu, Joseph E.  
 624 Gonzalez, Hao Zhang, and Ion Stoica. Efficient memory management for large language model  
 625 serving with pagedattention. In *Proceedings of the ACM SIGOPS 29th Symposium on Operating  
 626 Systems Principles*, 2023.

627

628 Yingyan Li, Lue Fan, Jiawei He, Yuqi Wang, Yuntao Chen, Zhaoxiang Zhang, and Tieniu  
 629 Tan. Enhancing end-to-end autonomous driving with latent world model. *arXiv preprint*  
 630 *arXiv:2406.08481*, 2024a.

631

632 Yingyan Li, Yuqi Wang, Yang Liu, Jiawei He, Lue Fan, and Zhaoxiang Zhang. End-to-end driving  
 633 with online trajectory evaluation via bev world model. *arXiv preprint arXiv:2504.01941*, 2025.

634

635 Zhenxin Li, Kailin Li, Shihao Wang, Shiyi Lan, Zhiding Yu, Yishen Ji, Zhiqi Li, Ziyue Zhu, Jan  
 636 Kautz, Zuxuan Wu, et al. Hydra-mdp: End-to-end multimodal planning with multi-target hydra-  
 637 distillation. *arXiv preprint arXiv:2406.06978*, 2024b.

638

639 Zhiqi Li, Wenhai Wang, Hongyang Li, Enze Xie, Chonghao Sima, Tong Lu, Qiao Yu, and Jifeng  
 640 Dai. Bevformer: learning bird’s-eye-view representation from lidar-camera via spatiotemporal  
 641 transformers. *IEEE Transactions on Pattern Analysis and Machine Intelligence*, 2024c.

642

643 Zhiqi Li, Zhiding Yu, Shiyi Lan, Jiahua Li, Jan Kautz, Tong Lu, and Jose M Alvarez. Is ego status  
 644 all you need for open-loop end-to-end autonomous driving? In *Proceedings of the IEEE/CVF*  
 645 *Conference on Computer Vision and Pattern Recognition*, pp. 14864–14873, 2024d.

646

647 Tingting Liang, Hongwei Xie, Kaicheng Yu, Zhongyu Xia, Zhiwei Lin, Yongtao Wang, Tao Tang,  
 648 Bing Wang, and Zhi Tang. Bevfusion: A simple and robust lidar-camera fusion framework.  
 649 *Advances in Neural Information Processing Systems*, 35:10421–10434, 2022.

650

651 Bencheng Liao, Shaoyu Chen, Haoran Yin, Bo Jiang, Cheng Wang, Sixu Yan, Xinbang Zhang,  
 652 Xiangyu Li, Ying Zhang, Qian Zhang, et al. Diffusiondrive: Truncated diffusion model for end-  
 653 to-end autonomous driving. In *Proceedings of the Computer Vision and Pattern Recognition*  
 654 *Conference*, pp. 12037–12047, 2025.

648 Haochen Liu, Zhiyu Huang, Wenhui Huang, Haohan Yang, Xiaoyu Mo, and Chen Lv. Hybrid-  
 649 prediction integrated planning for autonomous driving. *IEEE Transactions on Pattern Analysis  
 650 and Machine Intelligence*, 2025.

651 Srikant Malla, Chiho Choi, Isht Dwivedi, Joon Hee Choi, and Jiachen Li. Drama: Joint risk  
 652 localization and captioning in driving. In *Proceedings of the IEEE/CVF winter conference on  
 653 applications of computer vision*, pp. 1043–1052, 2023.

654 Jiageng Mao, Yuxi Qian, Junjie Ye, Hang Zhao, and Yue Wang. Gpt-driver: Learning to drive with  
 655 gpt. *arXiv preprint arXiv:2310.01415*, 2023.

656 Ana-Maria Marcu, Long Chen, Jan Hünermann, Alice Karnsund, Benoit Hanotte, Prajwal Chi-  
 657 dananda, Saurabh Nair, Vijay Badrinarayanan, Alex Kendall, Jamie Shotton, et al. Lingoqa: Vi-  
 658 sual question answering for autonomous driving. In *European Conference on Computer Vision*,  
 659 pp. 252–269. Springer, 2024.

660 Aditya Prakash, Kashyap Chitta, and Andreas Geiger. Multi-modal fusion transformer for end-to-  
 661 end autonomous driving. In *Proceedings of the IEEE/CVF conference on computer vision and  
 662 pattern recognition*, pp. 7077–7087, 2021.

663 Tianwen Qian, Jingjing Chen, Linhai Zhuo, Yang Jiao, and Yu-Gang Jiang. Nuscenes-qa: A multi-  
 664 modal visual question answering benchmark for autonomous driving scenario. In *Proceedings of  
 665 the AAAI Conference on Artificial Intelligence*, volume 38, pp. 4542–4550, 2024.

666 Zhihong Shao, Peiyi Wang, Qihao Zhu, Runxin Xu, Junxiao Song, Xiao Bi, Haowei Zhang,  
 667 Mingchuan Zhang, YK Li, Yang Wu, et al. Deepseekmath: Pushing the limits of mathemati-  
 668 cal reasoning in open language models. *arXiv preprint arXiv:2402.03300*, 2024.

669 Shaoshuai Shi, Li Jiang, Dengxin Dai, and Bernt Schiele. Mtr++: Multi-agent motion prediction  
 670 with symmetric scene modeling and guided intention querying. *IEEE Transactions on Pattern  
 671 Analysis and Machine Intelligence*, 46(5):3955–3971, 2024.

672 Chonghao Sima, Katrin Renz, Kashyap Chitta, Li Chen, Hanxue Zhang, Chengen Xie, Jens  
 673 Beßwenger, Ping Luo, Andreas Geiger, and Hongyang Li. Drivelm: Driving with graph vi-  
 674 sual question answering. In *European conference on computer vision*, pp. 256–274. Springer,  
 675 2024.

676 Ruiqi Song, Xianda Guo, Hangbin Wu, Qinggong Wei, and Long Chen. Insightdrive: Insight scene  
 677 representation for end-to-end autonomous driving. *arXiv preprint arXiv:2503.13047*, 2025.

678 Xiaolong Tang, Meina Kan, Shiguang Shan, and Xilin Chen. Plan-r1: Safe and feasible trajectory  
 679 planning as language modeling. *arXiv preprint arXiv:2505.17659*, 2025.

680 Xiaoyu Tian, Junru Gu, Bailin Li, Yicheng Liu, Yang Wang, Zhiyong Zhao, Kun Zhan, Peng Jia,  
 681 Xianpeng Lang, and Hang Zhao. Drivevlm: The convergence of autonomous driving and large  
 682 vision-language models. *arXiv preprint arXiv:2402.12289*, 2024.

683 Shihao Wang, Zhiding Yu, Xiaohui Jiang, Shiyi Lan, Min Shi, Nadine Chang, Jan Kautz, Ying Li,  
 684 and Jose M Alvarez. Omnidrive: A holistic llm-agent framework for autonomous driving with 3d  
 685 perception, reasoning and planning. *CoRR*, 2024.

686 Xinshuo Weng, Boris Ivanovic, Yan Wang, Yue Wang, and Marco Pavone. Para-drive: Parallelized  
 687 architecture for real-time autonomous driving. In *Proceedings of the IEEE/CVF Conference on  
 688 Computer Vision and Pattern Recognition*, pp. 15449–15458, 2024.

689 Dongming Wu, Wencheng Han, Yingfei Liu, Tiancai Wang, Cheng-zhong Xu, Xiangyu Zhang, and  
 690 Jianbing Shen. Language prompt for autonomous driving. In *Proceedings of the AAAI Conference  
 691 on Artificial Intelligence*, volume 39, pp. 8359–8367, 2025.

692 Shuo Xing, Chengyuan Qian, Yiping Wang, Hongyuan Hua, Kexin Tian, Yang Zhou, and  
 693 Zhengzhong Tu. Opennemma: Open-source multimodal model for end-to-end autonomous driv-  
 694 ing. In *Proceedings of the Winter Conference on Applications of Computer Vision*, pp. 1001–1009,  
 695 2025.

702 Yi Xu, Yuxin Hu, Zaiwei Zhang, Gregory P Meyer, Siva Karthik Mustikovela, Siddhartha Srinivasa,  
 703 Eric M Wolff, and Xin Huang. Vlm-ad: End-to-end autonomous driving through vision-language  
 704 model supervision. *arXiv preprint arXiv:2412.14446*, 2024.

705 Chengran Yuan, Zhanqi Zhang, Jiawei Sun, Shuo Sun, Zefan Huang, Christina Dao Wen Lee, Don-  
 706 gen Li, Yuhang Han, Anthony Wong, Keng Peng Tee, et al. Drama: An efficient end-to-end  
 707 motion planner for autonomous driving with mamba. *arXiv preprint arXiv:2408.03601*, 2024.

708 Zhenlong Yuan, Jing Tang, Jinguo Luo, Rui Chen, Chengxuan Qian, Lei Sun, Xiangxiang Chu,  
 709 Yujun Cai, Dapeng Zhang, and Shuo Li. Autodrive-r<sup>2</sup>: Incentivizing reasoning and self-reflection  
 710 capacity for vla model in autonomous driving. *arXiv preprint arXiv:2509.01944*, 2025.

711 Jingyi Zhang, Jiaxing Huang, Huanjin Yao, Shunyu Liu, Xikun Zhang, Shijian Lu, and Dacheng  
 712 Tao. R1-vl: Learning to reason with multimodal large language models via step-wise group  
 713 relative policy optimization. *arXiv preprint arXiv:2503.12937*, 2025.

714 Xingcheng Zhou, Xuyuan Han, Feng Yang, Yunpu Ma, and Alois C Knoll. Opendrivevla: To-  
 715 wards end-to-end autonomous driving with large vision language action model. *arXiv preprint  
 716 arXiv:2503.23463*, 2025a.

717 Zewei Zhou, Tianhui Cai, Seth Z Zhao, Yun Zhang, Zhiyu Huang, Bolei Zhou, and Jiaqi Ma. Au-  
 718 tovla: A vision-language-action model for end-to-end autonomous driving with adaptive reason-  
 719 ing and reinforcement fine-tuning. *arXiv preprint arXiv:2506.13757*, 2025b.

720 Zikang Zhou, Zihao Wen, Jianping Wang, Yung-Hui Li, and Yu-Kai Huang. Qcnext:  
 721 A next-generation framework for joint multi-agent trajectory prediction. *arXiv preprint  
 722 arXiv:2306.10508*, 2023.

723

724

725

726

727

728

729

730

731

732

733

734

735

736

737

738

739

740

741

742

743

744

745

746

747

748

749

750

751

752

753

754

755

756 

## A A USE OF LARGE LANGUAGE MODELS

757  
 758 We acknowledge the use of Large Language Models to assist in the preparation of this manuscript.  
 759 We utilize Google’s Gemini 2.5 Pro and DeepSeek-R1 for writing assistance. The specific applica-  
 760 tions are as follows:

761  
 762 • **Language and Readability:** To improve the grammar, clarity, and overall readability of  
 763 the manuscript through language polishing.  
 764 • **Format Checking:** Gemini 2.5 Pro and DeepSeek-R1 are used to aid in improving gram-  
 765 matical fluency, and enhancing the overall readability of the text.

766 We emphasize that all scientific claims, hypotheses, experimental designs, results, analyses, and  
 767 final conclusions are meticulously formulated, reviewed, and verified by the human authors. The  
 768 authors take full and final responsibility for the entire content of this submission, in accordance with  
 769 the ICLR policy.

770 

## B $P^3$ -*CoT* DATASET

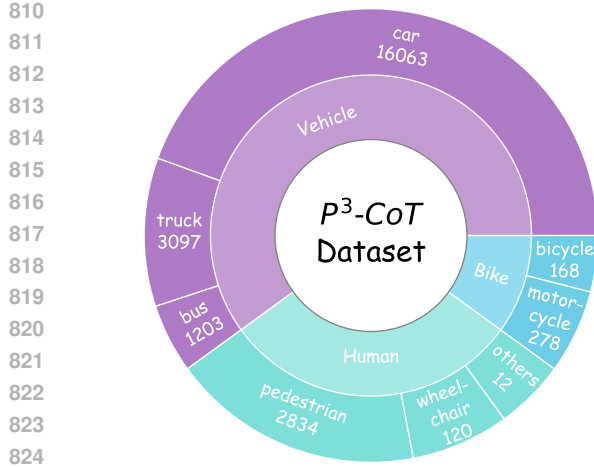
771  
 772 In this section, we will provide a detailed introduction to  $P^3$ -*CoT* dataset, including motivation,  
 773 data collection, data composition and distribution and comparisons between datasets.

774 

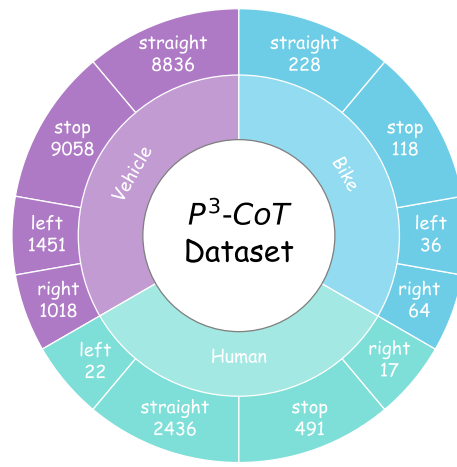
### B.1 MOTIVATION

775 The ultimate goal of autonomous driving models is to drive like humans. This target places high  
 776 demands on models, requiring them to understand the driving environment and think like humans.  
 777 Human drivers habitually identify and locate key objects that have a significant impact on driving  
 778 decisions and actions during the driving, and subconsciously predict their future behaviors to help  
 779 make the final driving routes. With deeper insight into autonomous driving models, the transforma-  
 780 tion of model architecture has undergone a shift from phased perception, prediction and planning to a  
 781 unified end-to-end structure. Though end-to-end structures gradually become mainstream due to the  
 782 reduction of accumulative errors, segmented consideration of perception, prediction and planning  
 783 remains a core design concept when designing new modules. Meanwhile, in the process of hu-  
 784 man understanding the driving environment, paying too much attention to unimportant objects will  
 785 instead reduce the concentration of human drivers and lead to unsafe driving behaviors. In other  
 786 words, focusing only on key objects is necessary for efficient and safe driving behaviors, which is  
 787 the same for the models. Considering the high requirements of comprehensive scene understanding  
 788 ability and complex logical decision-making capability in autonomous driving, the vision language  
 789 model (VLM) and reinforcement post-training show great potential. To cover all the thinking steps  
 790 of human drivers and meet the need of VLMs, a high quality reasoning dataset with key objects  
 791 and detailed CoT annotations is strongly recommended. This dataset should only focus on key ob-  
 792 jects and ignore unnecessary objects identification and localization, and construct a unified chain of  
 793 thought (CoT) including perception, prediction and planning.

794 However, the existing datasets can not meet such requirements. Some object grounding datasets  
 795 (Caesar et al., 2020) have been proposed to meet the need for fine-tuning VLMs in autonomous  
 796 driving perception tasks, but too many objects requiring grounding will introduce additional noises  
 797 as mentioned before. Existing approaches (Ding et al., 2024) attempt to establish chain of thought  
 798 datasets to supervised fine-tuning VLMs, and some of them recognize the special meaning of key  
 799 objects. These efforts only provide general descriptions of driving conditions, while overlooking the  
 800 necessity of considering the driving process in stages and the connection between different stages.  
 801 DriveLM (Sima et al., 2024) points out the importance of key objects and notices the significance  
 802 of the connection among different thinking steps. But DriveLM lacks a clear definition of key  
 803 objects and their impacts, and the annotations of DriveLM-nuScenes are incomplete both in key  
 804 frame selection and key object localization. Moreover, though DriveLM uses graph to model the  
 805 connection among the three stages of perception, prediction and planning, it formulates the data  
 806 as question-answer pairs which do not match the labels used in the CoT format and remains fixed  
 807 content templates lacking sufficient flexibility and diversity. Therefore, the following key challenges  
 808 remain to be addressed: 1) lack of completed and comprehensive key object annotations, 2) require-



825  
826  
827  
828  
829  
830  
831  
832  
833  
834  
Figure 7: The distribution of categories on  
P<sup>3</sup>-CoT (nuScenes).



825  
826  
827  
828  
829  
830  
831  
832  
833  
834  
Figure 8: The distribution of actions on  
P<sup>3</sup>-CoT (nuScenes).

830  
831  
832  
833  
834  
835  
836  
837  
838  
839  
840  
841  
842  
843  
844  
845  
846  
847  
848  
849  
850  
851  
852  
853  
854  
855  
856  
857  
858  
859  
860  
861  
862  
863

ments of unified chain of thought datasets for perception, prediction and planning, 3) a proper CoT format suitable for VLM training instead of question-and-answer pairs.

## B.2 DATA COLLECTION

To address these issues, we propose  $P^3$ -CoT dataset, a high-quality CoT dataset designed for VLM training and GRPO post-training. We first clarify significant concepts in our datasets. The key object of a specific scene is defined as those that human drivers will pay special attention in order to prevent potential dangerous events. This definition aims to simulate the attention of human driving, thereby aligning the model’s focus with that of human drivers. The concepts of stages in our dataset are similar to end-to-end autonomous driving. The perception stage asks the model to localize targets in RGB images, but only key objects; the prediction stage utilizes the results from the perception stage to reason the future behaviors of key objects; the planning stage accepts the objects and corresponding actions from the first two stages and obtains the final waypoints after comprehensive consideration. To construct  $P^3$  dataset, we first sample key frames of every scene in 2Hz following nuScenes settings, with 3 seconds history information as input and 3 seconds future trajectory as ground truth, and all the bounding boxes of objects will be projected into the image view. Considering that the distance between objects and ego car is an important factor in driving safety, we first filter out objects that are too far away and manually check the left objects to ensure high-quality key object annotations. It is worth noticing that we allow manual annotation of new objects that do not exist in previous dataset. After getting the key object annotations, we use trajectories of corresponding objects to determine future behaviors of objects in general directions like left or right and manually add the same labels according to videos if the object does not match any trajectory. And the way points in the future 3 seconds will be converted to the ego car coordinates as the ground truth. Given labels of the three stages and 3 seconds history information, we use the advanced Qwen2.5-VL-72B model to synthesize chain-of-thought data and make sure that only the results appearing in the previous stage can be used in the next stage to model the connections between different stages. The pipeline is shown in Fig. 3. Employing this annotation pipeline, we organize a high-quality and comprehensive CoT dataset with key object annotation and a unified perception-prediction-planning architecture in CoT format.  $P^3$ -CoT includes 19284 frames from 700 scenes in training set and 6019 frames from 150 scenes in test set based on nuScenes, and 103288 frames from 1192 scenes in training set and 12146 frames from 136 scenes in test set based on NAVSIM. With enough amount of CoT data,  $P^3$ -CoT dataset can support VLM training for both supervised fine-tuning and reinforcement post-training, and benefit from the connections among stages, VLM trained by the dataset can gain advantages both from staged thought process and lower accumulated error of end-to-end autonomous driving, which also brings additional explainability to the black box in autonomous driving.

864  
 865 Table 6: **The number of key objects in each frame of  $P^3\text{-}CoT$ .** The numbers on the table head  
 866 are the number of key objects in each frame. Average is calculated as total number of key objects  
 867 divided by total number of frames.

868 <b>Dataset</b>	<b>0</b>	<b>1</b>	<b>2</b>	<b>3</b>	<b>4</b>	<b>&gt;4</b>	<b>Average</b>
869 $P^3\text{-}CoT$ (nuScenes)	8187	9926	5121	1081	76	12	0.97
870 $P^3\text{-}CoT$ (NAVSIM)	24675	22915	20172	20794	20793	6085	2.08

872  
 873 Table 7: **The distribution of prediction actions of  $P^3\text{-}CoT$  (NAVSIM).** The number of position  
 874 of key objects in longitudinal and horizontal direction.

875 <b><math>P^3\text{-}CoT</math> (NAVSIM)</b>	<b>Left</b>	<b>Front</b>	<b>Right</b>
877 <b>Far</b>	7915	46909	4530
878 <b>Middle</b>	10601	33908	6558
879 <b>Near</b>	41435	31219	47815
880 <b>Behind</b>		9137	

### 883 B.3 DATA COMPOSITION

885  $P^3\text{-}CoT$  is composed of a training set of 19284 frames and a validation set of 5119 frames, attached  
 886 with detailed annotations for perception, prediction and planning three stages with connection.

887 For perception stage, we have tallied up the number of key objects that occur in each frame in Table  
 888 6 and the distribution of future actions of objects in Fig. 8 and the distribution of categories in  
 889 Fig. 7. Considering the relatively simple road conditions of the nuScenes dataset, the key objects  
 890 gathered from each frame should be sparse. The results listed in Table 6 show that our pipeline for  
 891 selecting key objects is reasonable and successfully reduces the additional and unnecessary objects  
 892 in the scene. The distribution of categories presents the diversity of  $P^3\text{-}CoT$  and that of actions is  
 893 in line with the situation in reality.

894 For prediction stage and planning stage, we annotate the future action of every object, including  
 895 the ego vehicle and other vehicles, and give the detailed results in Table 8, Table 7 and Fig. 8.  
 896 For nuScenes, future actions of prediction stage and planning stage have a similar distribution, but  
 897 the action straight of planning stage is more than that of prediction stage due to requirements of  
 898 data collection. For NAVSIM, we keep the same command types as nuScenes and adapt prediction  
 899 action types to NAVSIM. The actions of objects in NAVSIM focus on near range and front direction,  
 900 showing the complexity of NAVSIM in our settings.

### 901 B.4 COMPARISONS BETWEEN DATASETS

902 To highlight the advantages of  $P^3\text{-}CoT$  dataset, we give comprehensive comparisons of our dataset  
 903 and others in Table 9. We can tell from the table that  $P^3\text{-}CoT$  dataset annotates a substantial  
 904 number of frames and includes perception, prediction and planning all three stages. Unlike other  
 905 datasets,  $P^3\text{-}CoT$  formulates the data in CoT format and maintains the close connection among  
 906 stages, owning the special advantages to combine both staged interpretation and unified training  
 907 process.

### 910 B.5 DATA QUALITY ASSESSMENT

911 To ensure the high quality of the  $P^3\text{-}CoT$  dataset, we adopt a manual assessment protocol through  
 912 sampling inspection, following DriveLM (Sima et al., 2024). The evaluation is conducted at both  
 913 holistic and modular levels. At the holistic level, each CoT label is manually inspected to ensure it  
 914 strictly follows the prescribed reasoning structure—progressing completely and sequentially from  
 915 perception to prediction and then to planning, with all final module outputs present and correctly  
 916 formatted. At the modular level, we perform a fine-grained manual check for factual consistency  
 917 and reasoning quality. The dataset is divided into 10 splits, each assigned to three independent anno-

918  
919  
920  
921  
922  
923  
924  
925  
926 **Table 8: The distribution of planning commands in  $P^3\text{-CoT}$ .** The number of planning commands  
927 of ego vehicle.

Planning Commands	Left	Right	Stop	Straight
$P^3\text{-CoT}$ (nuScenes)	1299	1627	4919	16558
$P^3\text{-CoT}$ (NAVSIM)	27293	13524	1832	72785

926  
927  
928  
929 **Table 9: The comparisons of existing datasets of scale and structure.** Source Dataset: Source of  
930 data sampled. Frames: the number of frames labeled by methods. Perception, Prediction, Planning:  
931 whether the dataset includes the information about perception, prediction and planning. Type: data  
932 organization format.

Dataset	Source Dataset	Frames	Perception	Prediction	Planning	Type
nuScenes-QA (Qian et al., 2024)	nuScenes	34149	✓	✗	✗	QA
nuInstruct (Ding et al., 2024)	nuScenes	11850	✓	✓	✓	QA
nuPrompt (Wu et al., 2025)	nuScenes	34149	✓	✗	✗	QA
DriveLM-nuScenes (Sima et al., 2024)	nuScenes	4871	✓	✓	✓	QA
LingoQA (Marcu et al., 2024)	LingoQA	28000	—	—	—	QA
DRAMA (Malla et al., 2023)	DRAMA	17785	✓	✗	✓	QA
$P^3\text{-CoT}$ (Ours)	nuScenes	24403	✓	✓	✓	CoT+Label

933  
934  
935  
936  
937  
938  
939  
940  
941  
942  
943  
944  
945  
946  
947  
948  
949  
950  
951  
952  
953  
954  
955  
956  
957  
958  
959  
960  
961  
962  
963  
964  
965  
966  
967  
968  
969  
970  
971  
972  
973  
974  
975  
976  
977  
978  
979  
980  
981  
982  
983  
984  
985  
986  
987  
988  
989  
990  
991  
992  
993  
994  
995  
996  
997  
998  
999  
1000  
1001  
1002  
1003  
1004  
1005  
1006  
1007  
1008  
1009  
1010  
1011  
1012  
1013  
1014  
1015  
1016  
1017  
1018  
1019  
1020  
1021  
1022  
1023  
1024  
1025  
1026  
1027  
1028  
1029  
1030  
1031  
1032  
1033  
1034  
1035  
1036  
1037  
1038  
1039  
1040  
1041  
1042  
1043  
1044  
1045  
1046  
1047  
1048  
1049  
1050  
1051  
1052  
1053  
1054  
1055  
1056  
1057  
1058  
1059  
1060  
1061  
1062  
1063  
1064  
1065  
1066  
1067  
1068  
1069  
1070  
1071  
1072  
1073  
1074  
1075  
1076  
1077  
1078  
1079  
1080  
1081  
1082  
1083  
1084  
1085  
1086  
1087  
1088  
1089  
1090  
1091  
1092  
1093  
1094  
1095  
1096  
1097  
1098  
1099  
1100  
1101  
1102  
1103  
1104  
1105  
1106  
1107  
1108  
1109  
1110  
1111  
1112  
1113  
1114  
1115  
1116  
1117  
1118  
1119  
1120  
1121  
1122  
1123  
1124  
1125  
1126  
1127  
1128  
1129  
1130  
1131  
1132  
1133  
1134  
1135  
1136  
1137  
1138  
1139  
1140  
1141  
1142  
1143  
1144  
1145  
1146  
1147  
1148  
1149  
1150  
1151  
1152  
1153  
1154  
1155  
1156  
1157  
1158  
1159  
1160  
1161  
1162  
1163  
1164  
1165  
1166  
1167  
1168  
1169  
1170  
1171  
1172  
1173  
1174  
1175  
1176  
1177  
1178  
1179  
1180  
1181  
1182  
1183  
1184  
1185  
1186  
1187  
1188  
1189  
1190  
1191  
1192  
1193  
1194  
1195  
1196  
1197  
1198  
1199  
1200  
1201  
1202  
1203  
1204  
1205  
1206  
1207  
1208  
1209  
1210  
1211  
1212  
1213  
1214  
1215  
1216  
1217  
1218  
1219  
1220  
1221  
1222  
1223  
1224  
1225  
1226  
1227  
1228  
1229  
1230  
1231  
1232  
1233  
1234  
1235  
1236  
1237  
1238  
1239  
1240  
1241  
1242  
1243  
1244  
1245  
1246  
1247  
1248  
1249  
1250  
1251  
1252  
1253  
1254  
1255  
1256  
1257  
1258  
1259  
1260  
1261  
1262  
1263  
1264  
1265  
1266  
1267  
1268  
1269  
1270  
1271  
1272  
1273  
1274  
1275  
1276  
1277  
1278  
1279  
1280  
1281  
1282  
1283  
1284  
1285  
1286  
1287  
1288  
1289  
1290  
1291  
1292  
1293  
1294  
1295  
1296  
1297  
1298  
1299  
1300  
1301  
1302  
1303  
1304  
1305  
1306  
1307  
1308  
1309  
1310  
1311  
1312  
1313  
1314  
1315  
1316  
1317  
1318  
1319  
1320  
1321  
1322  
1323  
1324  
1325  
1326  
1327  
1328  
1329  
1330  
1331  
1332  
1333  
1334  
1335  
1336  
1337  
1338  
1339  
1340  
1341  
1342  
1343  
1344  
1345  
1346  
1347  
1348  
1349  
1350  
1351  
1352  
1353  
1354  
1355  
1356  
1357  
1358  
1359  
1360  
1361  
1362  
1363  
1364  
1365  
1366  
1367  
1368  
1369  
1370  
1371  
1372  
1373  
1374  
1375  
1376  
1377  
1378  
1379  
1380  
1381  
1382  
1383  
1384  
1385  
1386  
1387  
1388  
1389  
1390  
1391  
1392  
1393  
1394  
1395  
1396  
1397  
1398  
1399  
1400  
1401  
1402  
1403  
1404  
1405  
1406  
1407  
1408  
1409  
1410  
1411  
1412  
1413  
1414  
1415  
1416  
1417  
1418  
1419  
1420  
1421  
1422  
1423  
1424  
1425  
1426  
1427  
1428  
1429  
1430  
1431  
1432  
1433  
1434  
1435  
1436  
1437  
1438  
1439  
1440  
1441  
1442  
1443  
1444  
1445  
1446  
1447  
1448  
1449  
1450  
1451  
1452  
1453  
1454  
1455  
1456  
1457  
1458  
1459  
1460  
1461  
1462  
1463  
1464  
1465  
1466  
1467  
1468  
1469  
1470  
1471  
1472  
1473  
1474  
1475  
1476  
1477  
1478  
1479  
1480  
1481  
1482  
1483  
1484  
1485  
1486  
1487  
1488  
1489  
1490  
1491  
1492  
1493  
1494  
1495  
1496  
1497  
1498  
1499  
1500  
1501  
1502  
1503  
1504  
1505  
1506  
1507  
1508  
1509  
1510  
1511  
1512  
1513  
1514  
1515  
1516  
1517  
1518  
1519  
1520  
1521  
1522  
1523  
1524  
1525  
1526  
1527  
1528  
1529  
1530  
1531  
1532  
1533  
1534  
1535  
1536  
1537  
1538  
1539  
1540  
1541  
1542  
1543  
1544  
1545  
1546  
1547  
1548  
1549  
1550  
1551  
1552  
1553  
1554  
1555  
1556  
1557  
1558  
1559  
1560  
1561  
1562  
1563  
1564  
1565  
1566  
1567  
1568  
1569  
1570  
1571  
1572  
1573  
1574  
1575  
1576  
1577  
1578  
1579  
1580  
1581  
1582  
1583  
1584  
1585  
1586  
1587  
1588  
1589  
1590  
1591  
1592  
1593  
1594  
1595  
1596  
1597  
1598  
1599  
1600  
1601  
1602  
1603  
1604  
1605  
1606  
1607  
1608  
1609  
1610  
1611  
1612  
1613  
1614  
1615  
1616  
1617  
1618  
1619  
1620  
1621  
1622  
1623  
1624  
1625  
1626  
1627  
1628  
1629  
1630  
1631  
1632  
1633  
1634  
1635  
1636  
1637  
1638  
1639  
1640  
1641  
1642  
1643  
1644  
1645  
1646  
1647  
1648  
1649  
1650  
1651  
1652  
1653  
1654  
1655  
1656  
1657  
1658  
1659  
1660  
1661  
1662  
1663  
1664  
1665  
1666  
1667  
1668  
1669  
1670  
1671  
1672  
1673  
1674  
1675  
1676  
1677  
1678  
1679  
1680  
1681  
1682  
1683  
1684  
1685  
1686  
1687  
1688  
1689  
1690  
1691  
1692  
1693  
1694  
1695  
1696  
1697  
1698  
1699  
1700  
1701  
1702  
1703  
1704  
1705  
1706  
1707  
1708  
1709  
1710  
1711  
1712  
1713  
1714  
1715  
1716  
1717  
1718  
1719  
1720  
1721  
1722  
1723  
1724  
1725  
1726  
1727  
1728  
1729  
1730  
1731  
1732  
1733  
1734  
1735  
1736  
1737  
1738  
1739  
1740  
1741  
1742  
1743  
1744  
1745  
1746  
1747  
1748  
1749  
1750  
1751  
1752  
1753  
1754  
1755  
1756  
1757  
1758  
1759  
1760  
1761  
1762  
1763  
1764  
1765  
1766  
1767  
1768  
1769  
1770  
1771  
1772  
1773  
1774  
1775  
1776  
1777  
1778  
1779  
1780  
1781  
1782  
1783  
1784  
1785  
1786  
1787  
1788  
1789  
1790  
1791  
1792  
1793  
1794  
1795  
1796  
1797  
1798  
1799  
1800  
1801  
1802  
1803  
1804  
1805  
1806  
1807  
1808  
1809  
1810  
1811  
1812  
1813  
1814  
1815  
1816  
1817  
1818  
1819  
1820  
1821  
1822  
1823  
1824  
1825  
1826  
1827  
1828  
1829  
1830  
1831  
1832  
1833  
1834  
1835  
1836  
1837  
1838  
1839  
1840  
1841  
1842  
1843  
1844  
1845  
1846  
1847  
1848  
1849  
1850  
1851  
1852  
1853  
1854  
1855  
1856  
1857  
1858  
1859  
1860  
1861  
1862  
1863  
1864  
1865  
1866  
1867  
1868  
1869  
1870  
1871  
1872  
1873  
1874  
1875  
1876  
1877  
1878  
1879  
1880  
1881  
1882  
1883  
1884  
1885  
1886  
1887  
1888  
1889  
1890  
1891  
1892  
1893  
1894  
1895  
1896  
1897  
1898  
1899  
1900  
1901  
1902  
1903  
1904  
1905  
1906  
1907  
1908  
1909  
1910  
1911  
1912  
1913  
1914  
1915  
1916  
1917  
1918  
1919  
1920  
1921  
1922  
1923  
1924  
1925  
1926  
1927  
1928  
1929  
1930  
1931  
1932  
1933  
1934  
1935  
1936  
1937  
1938  
1939  
1940  
1941  
1942  
1943  
1944  
1945  
1946  
1947  
1948  
1949  
1950  
1951  
1952  
1953  
1954  
1955  
1956  
1957  
1958  
1959  
1960  
1961  
1962  
1963  
1964  
1965  
1966  
1967  
1968  
1969  
1970  
1971  
1972  
1973  
1974  
1975  
1976  
1977  
1978  
1979  
1980  
1981  
1982  
1983  
1984  
1985  
1986  
1987  
1988  
1989  
1990  
1991  
1992  
1993  
1994  
1995  
1996  
1997  
1998  
1999  
2000  
2001  
2002  
2003  
2004  
2005  
2006  
2007  
2008  
2009  
2010  
2011  
2012  
2013  
2014  
2015  
2016  
2017  
2018  
2019  
2020  
2021  
2022  
2023  
2024  
2025  
2026  
2027  
2028  
2029  
2030  
2031  
2032  
2033  
2034  
2035  
2036  
2037  
2038  
2039  
2040  
2041  
2042  
2043  
2044  
2045  
2046  
2047  
2048  
2049  
2050  
2051  
2052  
2053  
2054  
2055  
2056  
2057  
2058  
2059  
2060  
2061  
2062  
2063  
2064  
2065  
2066  
2067  
2068  
2069  
2070  
2071  
2072  
2073  
2074  
2075  
2076  
2077  
2078  
2079  
2080  
2081  
2082  
2083  
2084  
2085  
2086  
2087  
2088  
2089  
2090  
2091  
2092  
2093  
2094  
2095  
2096  
2097  
2098  
2099  
2100  
2101  
2102  
2103  
2104  
2105  
2106  
2107  
2108  
2109  
2110  
2111  
2112  
2113  
2114  
2115  
2116  
2117  
2118  
2119  
2120  
2121  
2122  
2123  
2124  
2125  
2126  
2127  
2128  
2129  
2130  
2131  
2132  
2133  
2134  
2135  
2136  
2137  
2138  
2139  
2140  
2141  
2142  
2143  
2144  
2145  
2146  
2147  
2148  
2149  
2150  
2151  
2152  
2153  
2154  
2155  
2156  
2157  
2158  
2159  
2160  
2161  
2162  
2163  
2164  
2165  
2166  
2167  
2168  
2169  
2170  
2171  
2172  
2173  
2174  
2175  
2176  
2177  
2178  
2179  
2180  
2181  
2182  
2183  
2184  
2185  
2186  
2187  
2188  
2189  
2190  
2191  
2192  
2193  
2194  
2195  
2196  
2197  
2198  
2199  
2200  
2201  
2202  
2203  
2204  
2205  
2206  
2207  
2208  
2209  
2210  
2211  
2212  
2213  
2214  
2215  
2216  
2217  
2218  
2219  
2220  
2221  
2222  
2223  
2224  
2225  
2226  
2227  
2228  
2229  
2230  
2231  
2232  
2233  
2234  
2235  
2236  
2237  
2238  
2239  
2240  
2241  
2242  
2243  
2244  
2245  
2246  
2247  
2248  
2249  
2250  
2251  
2252  
2253  
2254  
2255  
2256  
2257  
2258  
2259  
2260  
2261  
2262  
2263  
2264  
2265  
2266  
2267  
2268  
2269  
2270  
2271  
2272  
2273  
2274  
2275  
2276  
2277  
2278  
2279  
2280  
2281  
2282  
2283  
2284  
2285  
2286  
2287  
2288  
2289  
2290  
2291  
2292  
2293  
2294  
2295  
2296  
2297  
2298  
2299  
2300  
2301  
2302  
2303  
2304  
2305  
2306  
2307  
2308  
2309  
2310  
2311  
2312  
2313  
2314  
2315  
2316  
2317  
2318  
2319  
2320  
2321  
2322  
2323  
2324  
2325  
2326  
2327  
2328  
2329  
2330  
2331  
2332  
2333  
2334  
2335  
2336  
2337  
2338  
2339  
2340  
2341  
2342  
2343  
2344  
2345  
2346  
2347  
2348  
2349  
2350  
2351  
2352  
2353  
2354  
2355  
2356  
2357  
2358  
2359  
2360  
2361  
2362  
2363  
2364  
2365  
2366  
2367  
2368  
2369  
2370  
2371  
2372  
2373  
2374  
2375  
2376  
2377  
2378  
2379  
2380  
2381  
2382  
2383  
2384  
2385  
2386  
2387  
2388  
2389  
2390  
2391  
2392  
2393  
2394  
2395  
2396  
2397  
2398  
2399  
2400  
2401  
2402  
2403  
2404  
2405  
2406  
2407  
2408  
2409  
2410  
2411  
2412  
2413  
2414  
2415  
2416  
2417  
2418  
2419  
2420  
2421  
2422  
2423  
2424  
2425  
2426  
2427  
2428  
2429  
2430  
2431  
2432  
2433  
2434  
2435  
2436  
2437  
2438  
2439  
2440  
2441  
2442  
2443  
2444  
2445  
2446  
2447  
2448  
2449  
2450  
2451  
2452  
2453  
2454  
2455  
2456  
2457  
2458  
2459  
2460  
2461  
2462  
2463  
2464  
2465  
2466  
2467  
2468  
2469  
2470  
2471  
2472  
2473  
2474  
2475  
2476  
2477  
2478  
2479  
2480  
2481  
2482  
2483  
2484  
2485  
2486  
2487  
2488  
2489  
2490  
2491  
2492  
2493  
2494  
2495  
2496  
2497  
2498  
2499  
2500  
2501  
2502  
2503  
2504  
2505  
2506  
2507  
2508  
2509  
2510  
2511  
2512  
2513  
2514  
2515  
2516  
2517  
2518  
2519  
2520  
2521  
2522  
2523  
2524  
2525  
2526  
2527  
2528  
2529  
2530  
2531  
2532  
2533  
2534  
2535  
2536  
2537  
2538  
2539  
2540  
2541  
2542  
2543  
2544  
2545  
2546  
2547  
2548  
2549  
2550  
2551  
2552  
2553  
2554  
2555  
2556  
2557  
2558  
2559  
2560  
2561  
2562  
2563  
2564  
2565  
2566  
2567  
2568  
2569  
2570  
2571  
2572  
2573  
2574  
2575  
2576  
2577  
2578  
2579  
2580  
2581  
2582  
2583  
2584  
2585  
2586  
2587  
2588  
2589  
2590  
2591  
2592  
2593  
2594  
2595  
2596  
2597  
2598<br

972 and planning decisions. The reward function is carefully designed to integrate both spatial localization  
 973 accuracy and behavioral semantics:  
 974

$$975 \quad 976 \quad 977 \quad 978 \quad R_{\text{pred}} = \left( \frac{\sum_{(i,j) \in \mathcal{M}} \text{IoU}_{ij} \cdot \mathbb{I}(s_i = s_j)}{\sum_{(i,j) \in \mathcal{M}} \text{IoU}_{ij}} \right) \cdot (\text{IoU}_{\text{avg}} \cdot (0.5P + 0.5R)), \quad (14)$$

979 where  $\mathcal{M}$  represents the set of successfully matched prediction-ground truth pairs, and  $\mathbb{I}$  is the  
 980 indicator function that returns 1 when the predicted action label  $s_i$  matches the ground truth  $s_j$ , and  
 981 0 otherwise.

982 The formula consists of two multiplicative components. The first term calculates a weighted  
 983 behavior accuracy score, where each matched pair's label correctness is weighted by its IoU value.  
 984 This design ensures that predictions with better spatial alignment contribute more significantly to  
 985 the reward. The second term represents the fundamental detection quality, computed as the product  
 986 of average IoU and the F1-score (harmonic mean of precision and recall), which maintains the basic  
 987 requirement of accurate object detection and tracking.

988 This reward design serves two crucial purposes. First, it explicitly encodes the dependency between  
 989 accurate perception and reliable prediction - the model cannot achieve high prediction rewards with-  
 990 out first establishing solid perceptual foundations. Second, it emphasizes that behavioral prediction  
 991 quality is intrinsically tied to spatial accuracy; even correct action labels receive reduced rewards if  
 992 the associated bounding boxes are poorly localized.

993 By designing the prediction reward in this manner, we force the model to develop a comprehensive  
 994 understanding of scene dynamics, where it must not only identify objects correctly but also antic-  
 995 ipate their future behaviors accurately. This approach ensures that the prediction module provides  
 996 meaningful and reliable inputs to the planning system, enabling the generation of safe and efficient  
 997 driving strategies that account for the predicted evolution of the traffic environment.

998 **Planning Reward ( $R_{\text{plan}}$ ):** This component serves as the ultimate performance metric that evaluates  
 999 the quality of the ego vehicle's planned trajectory, representing the final output of the entire reason-  
 1000 ing pipeline. The reward is calculated through an exponential transformation of the L2 distance  
 1001 between the predicted trajectory points and their ground-truth counterparts:

$$1003 \quad 1004 \quad 1005 \quad R_{\text{plan}} = \frac{2}{1 + e^{\text{clip}(L2, 0, L2_{\text{max}})}}, \quad (15)$$

1006 where L2 represents the mean Euclidean distance between corresponding points in the predicted and  
 1007 ground-truth trajectories across all future time horizons. Following AutoVLA (Zhou et al., 2025b),  
 1008 we add PDMS to planning reward for NAVSIM benchmark.

1009 The planning reward serves as the ultimate validator of the entire  $P^3$  reasoning chain. While high  
 1010 rewards in perception and prediction are necessary prerequisites, they are insufficient without corre-  
 1011 sponding excellence in planning. This design explicitly teaches the model that accurate perception  
 1012 and reliable prediction are valuable precisely because they enable superior planning decisions. The  
 1013 planning reward thus creates a powerful end-to-end learning signal that backpropagates through all  
 1014 modules, encouraging the development of coordinated representations where each component works  
 1015 synergistically toward the final goal of generating safe, comfortable, and efficient driving trajec-  
 1016 tories.

1017 By placing the planning reward at the apex of our reward hierarchy, we ensure that the model opti-  
 1018 mizes not for intermediate metrics but for the ultimate objective of successful autonomous naviga-  
 1019 tion, while maintaining the interpretability and safety guarantees provided by the structured  $P^3$ - $COT$   
 1020 reasoning process.

1021 These rewards with  $P^3$ -GRPO algorithm ensure that improvements in planning performance are  
 1022 grounded in corresponding enhancements in perceptual understanding and predictive capability,  
 1023 creating a synergistic effect where each module's optimization contributes to the overall driving  
 1024 performance. The algorithm maintains the interpretability and safety guarantees provided by the  
 1025 structured  $P^3$ - $COT$  reasoning process while achieving superior autonomous driving performance  
 through multi-module reinforcement learning.

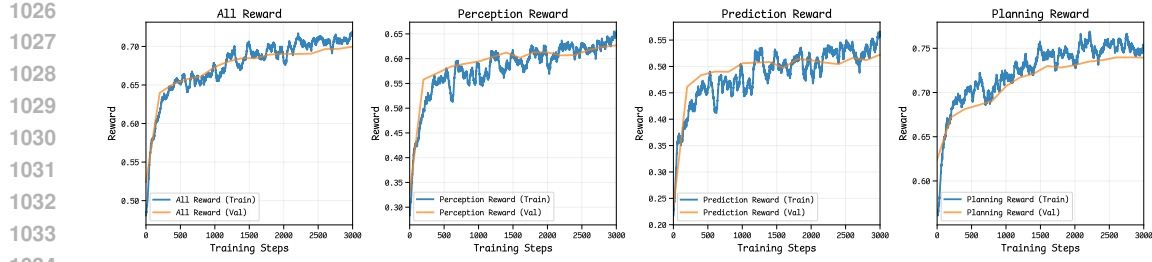


Figure 9: **Training and testing rewards for perception, prediction, planning, and all reward.** The results shows the consistent improvement in all rewards, which proves the tight inter-connection among three stages and the effectiveness of  $P^3$ -CoT.

**Reward Visualization.** We visualize the training and testing rewards for perception, prediction, planning, and the all reward, as shown in Fig. 9. The results demonstrate that through training with our  $P^3$ -CoT dataset and  $P^3$ -GRPO algorithm, the three modules exhibit mutual reinforcement, leading to consistent improvement in their respective rewards. This synergistic effect is particularly beneficial for planning performance, as the enhanced perception and prediction capabilities provide more reliable inputs for trajectory generation. The progressive optimization across modules ensures coherent reasoning and decision-making, ultimately contributing to more robust autonomous driving performance.

**Ablation Study on Reward Weight.** As shown in Table 10, we conduct additional ablation studies on three reward weight configurations. Results indicate that an unbalanced setting (e.g., 1:1:1:7), which overemphasizes the planning reward, can hinder the optimization of perception and prediction modules. This imbalance ultimately leads to inferior overall planning performance, as accurate planning is contingent upon reliable inputs from the preceding stages.

Table 10: **Weight Setting on nuScenes Benchmark.**

Reward weight	Perception $\uparrow$	Prediction $\uparrow$	Planning (Avg. L2) $\downarrow$
1:2:2:5	<b>0.64</b>	<b>0.54</b>	<b>0.33</b>
1:1:1:7	0.63	0.53	0.34

## D EXPERIMENTAL SETUP

We conduct experiments on two autonomous driving benchmarks: nuScenes and NAVSIM. The detailed experimental configurations are summarized in Table 11. For both datasets, we compare the Cold-Start baseline with our proposed  $P^3$ -GRPO approach under consistent data settings. We also perform an ablation experiment by removing the KL divergence term from the training objective. As demonstrated in Fig. 10, the model without KL regularization suffers from significant performance degradation as training progresses, eventually leading to model collapse. This occurs because the absence of KL constraint allows the model to deviate excessively from the base policy, resulting in unstable optimization. Therefore, we recommend retaining the KL divergence term during training to ensure the model maintains reasonable proximity to the base policy while improving performance.

## E QUALITATIVE COMPARISON OF TRAJECTORY PLANNING

To further explain the advantages of our method, we provide an intuitive comparison of the results in this section. For nuScenes samples, the red points denote ground truth trajectory, the orange denotes our trajectory with detail CoT, the pink denotes our trajectory with only CoT framework, the green denotes OmniDrive trajectory and the blue denotes VAD trajectory. For NAVSIM samples, the red points denote ground truth trajectory, the orange denotes our trajectory with detail CoT, the pink denotes our trajectory with only CoT framework, the green denotes WoTE trajectory and the blue denotes DiffusionDrive trajectory. Due to camera projection limitations, too short and too deviated trajectories will not appear in the images, such as stop situations. The CoT and answers corresponding to the specific sample are shown on the right of the figure.

Table 11: Experimental setup.

	nuScenes		NAVSIM	
	Cold-Start	$P^3\text{-GRPO}$	Cold-Start	$P^3\text{-GRPO}$
<b>Data Setting</b>				
Video Shape	[6, 3, 252, 448]	[6, 3, 252, 448]	[4, 3, 168, 672]	[4, 3, 168, 672]
History Traj	6	6	4	4
Future Traj	6	6	8	8
Ego Infos	Only $V$	Only $V$	$a_x, a_y, v_x, v_y$	$a_x, a_y, v_x, v_y$
<b>Optimization</b>				
Epoch	1	5	1	5
Batch size	8	256	8	256
Optimizer	AdamW	AdamW	AdamW	AdamW
Learning Rate	2e-5	1e-6	2e-5	1e-6
<b>GRPO Setting</b>				
Group Size	–	8	–	8
KL Weight	–	0.01	–	0.01

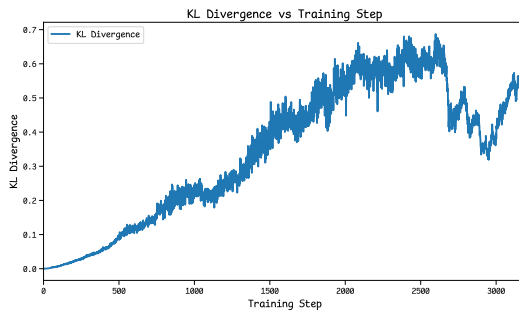


Figure 10: Ablation Study on KL Divergence.

In Fig. 11(a), the front view shows a scene at night with waiting cars. Due to image distortion, the street lamps have shifted towards the green light to a certain extent. The ground truth trajectory is to stop and wait, while the trajectories of comparison methods ignore the front car and move forward mistakenly. Our method first correctly observes the key objects, the closest two cars, and does not misunderstand the meaning of the lights, and then precisely gives the right future actions of the two. This result supports our planning decisions and our method finally takes the same actions as ground truth. This shows our method the powerful ability of scene understanding.

In Fig. 11(b), two trucks are parked by the roadside, and one of them blocks moving direction of the ego car. The ground truth trajectory still moves forward and tends to return to the initial road, but it seems too close to the truck on the right. The comparison methods do not work well in this sample. Our method can still identify key objects as before and provide good prediction answers. Though the trajectory is at a certain distance from the ground truth, we believe that our method takes into account the truck on the right to correct its initial decision and avoid potential security issues.

Except for the specific explanation of the samples, we also provide special cases with completed questions and answers in Fig. 12 to Fig. 17. The first two are nuScenes samples and the last four are NAVSIM samples.

```
1134
1135
1136
1137
1138
1139
1140
1141
1142
1143
1144
1145
1146
1147 <ours-fast>
1148   <think_perception> </think_perception> <answer_perception>```json\n[{\\"bbox_2d": "[182, 129, 316, 249], \"label": "l\\\"an\\\"a"}, {\\"bbox_2d": [307, 116, 448, 252], \"label": "l\\\"an\\\"a"}]\n```</answer_perception>
1149   <think_prediction> </think_prediction> <answer_prediction>```json\n[{\\"bbox_2d": "[182, 129, 316, 249], \"future_action": "straight"}, {\\"bbox_2d": [307, 116, 448, 252], \"future_action": "straight"}]\n```</answer_prediction>
1150   <think_planning> </think_planning> <answer_planning>```json\n[{\\"point_2d": [0.0, 0.0], \"label": "0.0s"}, {\\"point_2d": [0.0, 0.0], \"label": "1.5s"}, {\\"point_2d": [0.0, 0.0], \"label": "3.0s"}, {\\"point_2d": [0.0, 0.0], \"label": "2.5s"}]\n```</answer_planning>
```



OUR-DETAILED:

\think\_perception:Let's examine the image for key objects such as cars, buses, trucks, bicycles, pedestrians, and motorcycles. The image is dark, indicating it might be nighttime, and the road is visible with some greenery on the side.\n\nFirst, I need to identify the objects in the image. I see two cars clearly. The **first car** is in the center of the image, and the **second car** is on the right side.\n\nNext, I need to determine the coordinates of these objects. So I will estimate the bounding boxes for each car.\n\nFor the first car, it is centrally located. I estimate the bounding box coordinates as [182, 126, 315, 252]. For the second car, it is on the right side. I estimate the bounding box coordinates as [308, 114, 448, 248].\n\nThese bounding boxes represent the detected cars in the image.\n\nanswer\_perception: json\n "bbox\_2d": "[182, 126, 315, 252]",\n "label": "\ncar"\n},\n "bbox\_2d": "[308, 114, 448, 249]",\n "label": "\ncar"\n}\n}\n\n

\think\_perception:Let me think. We have two key objects, both labeled as cars. The first car, `<car>[182, 126, 315, 252]`, is currently stationary and not in the moving direction of the ego vehicle. The second car, `<car>[308, 114, 448, 249]`, is also stationary and not in the moving direction of the ego vehicle. Since both cars are stationary and there are no traffic lights, the future action for both cars is to remain stationary. Therefore, the prediction for the future action of both cars is 'stop'.\n\n\think\_projection:\n json\n "bbox\_2d": "[182, 126, 315, 252]",\n "future\_action": "stop"\n},\n "bbox\_2d": "[308, 114, 448, 249]",\n "future\_action": "stop"\n}\n}\n\n

\think\_planning:\n\nOh, I see. The ego vehicle is currently at 0.0 m/s, and the historical trajectory shows that it has been stationary for the last 3 seconds. The ego future action is to stop, and the key objects do not affect the ego vehicle. Since the ego vehicle is already stationary and the future action is to stop, the planned trajectory will remain at 0.0 m/s for the next 3 seconds.\n\nTo determine the planning trajectory, I will calculate the position at each 0.5-second interval for the next 3 seconds. Since the vehicle is stationary, the x and y values will remain at 0.0.\n\nLet's calculate the trajectory:\n- At 0.0s: [0.0, 0.0]\n- At 0.5s: [0.0, 0.0]\n- At 1.0s: [0.0, 0.0]\n- At 1.5s: [0.0, 0.0]\n- At 2.0s: [0.0, 0.0]\n- At 2.5s: [0.0, 0.0]\n- At 3.0s: [0.0, 0.0]\n\n\think\_planning:\n json\n "point\_2d": "[0.0, 0.0]",\n "label": "\n0.5s"\n},\n "point\_2d": "[0.0, 0.0]",\n "label": "\n1.0s"\n},\n "point\_2d": "[0.0, 0.0]",\n "label": "\n1.5s"\n},\n "point\_2d": "[0.0, 0.0]",\n "label": "\n2.0s"\n},\n "point\_2d": "[0.0, 0.0]",\n "label": "\n2.5s"\n},\n "point\_2d": "[0.0, 0.0]",\n "label": "\n3.0s"\n}\n\n

(a)



**OURS-DETAILED:**

<think\_perception> Let's examine the image for key objects such as cars, buses, trucks, bicycles, pedestrians, and motorcycles. The image size is 448x252 pixels. **I notice two trucks in the image. I need to determine the coordinates of each truck.** The first truck is on the left side of the image. I estimate its bounding box coordinates to be around (0, 60) to (150, 200). The second truck is on the right side of the image. I estimate its bounding box coordinates to be around (300, 100) to (448, 180). **Now, let's compile this information into the required format.** </think\_perception>

<answer\_perception> `json[{"bbox_2d": [0, 60, 150, 200], "label": "truck"}, {"bbox_2d": [300, 100, 448, 180], "label": "truck"}]` </answer\_perception>

<think\_prediction> Let me think. We have two trucks in the scene. The first truck, `truck[0]`, is stationary and not in the moving direction of the ego vehicle. The second truck, `truck[1]`, is stationary and in the moving direction of the ego vehicle. Since both trucks are stationary and there are no traffic lights, the future action for both trucks is to remain stationary. Therefore, the prediction for the future action of both trucks is `"stop"`. </think\_prediction>

<answer\_prediction> `json[{"bbox_2d": [0, 60, 150, 200], "future_action": "stop"}, {"bbox_2d": [300, 100, 448, 180], "future_action": "stop"}]` </answer\_prediction>

<think\_planning> Let me think. The ego vehicle's current speed is 0.66 m/s, and its future action is to go straight. The historical trajectory shows a consistent straight path with slight lateral deviations. The key objects in the scene are two trucks, which are not traffic lights. The ego vehicle can maintain its speed and direction. **Now to determine the planned trajectory.** We will update the ego vehicle's position at 0.66 m/s second interval for the next 3 seconds. The ego vehicle is moving straight, so the x-coordinate will remain close to zero, while the y-coordinate will increase based on the speed. **At 0.5s:** The vehicle moves 0.66 m/s \* 0.5s = 0.33 meters forward. **Adjusting for slight lateral deviation:** the x-coordinate is approximately 0.01. **At 1.0s:** The vehicle moves an additional 0.66 m/s \* 1.0s = 0.66 meters forward. Adjusting for lateral deviation, the x-coordinate is approximately 0.02. **At 1.5s:** The vehicle moves an additional 0.66 m/s \* 1.5s = 0.99 meters forward. **Adjusting for lateral deviation:** the x-coordinate is approximately 0.03. **At 2.0s:** The vehicle moves an additional 0.66 m/s \* 2.0s = 1.32 meters forward. **Adjusting for lateral deviation:** the x-coordinate is approximately 0.04. **At 2.5s:** The vehicle moves an additional 0.66 m/s \* 2.5s = 1.65 meters forward. **Adjusting for lateral deviation:** the x-coordinate is approximately 0.05. **At 3.0s:** The vehicle moves an additional 0.66 m/s \* 3.0s = 1.98 meters forward. **Adjusting for lateral deviation:** the x-coordinate is approximately 0.06. **In the planned trajectory:** the x-coordinate is approximately 0.01, 0.02, 0.03, 0.04, 0.05. **Now to determine the planned trajectory:** the y-coordinate is approximately 0.56, 0.62, 0.68, 0.74, 0.80. **At 0.5s:** The vehicle moves 0.66 m/s \* 0.5s = 0.33 meters forward. **Adjusting for slight lateral deviation:** the y-coordinate is approximately 0.56 + 0.33 = 0.89. **At 1.0s:** The vehicle moves an additional 0.66 m/s \* 1.0s = 0.66 meters forward. Adjusting for lateral deviation, the y-coordinate is approximately 0.89 + 0.66 = 1.55. **At 1.5s:** The vehicle moves an additional 0.66 m/s \* 1.5s = 0.99 meters forward. Adjusting for lateral deviation, the y-coordinate is approximately 1.55 + 0.99 = 2.54. **At 2.0s:** The vehicle moves an additional 0.66 m/s \* 2.0s = 1.32 meters forward. Adjusting for lateral deviation, the y-coordinate is approximately 2.54 + 1.32 = 3.86. **At 2.5s:** The vehicle moves an additional 0.66 m/s \* 2.5s = 1.65 meters forward. Adjusting for lateral deviation, the y-coordinate is approximately 3.86 + 1.65 = 5.51. **At 3.0s:** The vehicle moves an additional 0.66 m/s \* 3.0s = 1.98 meters forward. Adjusting for lateral deviation, the y-coordinate is approximately 5.51 + 1.98 = 7.49. **Final planned trajectory:** `json[{"point_2d": [0, 0.56], "label": "0.5s"}, {"point_2d": [0.01, 0.89], "label": "1.0s"}, {"point_2d": [0.02, 1.55], "label": "1.5s"}, {"point_2d": [0.03, 2.54], "label": "2.0s"}, {"point_2d": [0.04, 3.86], "label": "2.5s"}, {"point_2d": [0.05, 7.49], "label": "3.0s"}]` </think\_planning>

(b)

Figure 11: **Visualization examples of specific samples.** Every example is equipped with visualization of results on the top and CoT answer on the bottom.

1188  
 1189  
 1190  
 1191  
 1192  
 1193  
 1194  
 1195  
 1196  
 1197  
 1198  
 1199  
 1200  
 1201  
 1202  
 1203  
 1204  
 1205  
 1206  
 1207  
 1208  
 1209  
 1210  
 1211  
 1212  
 1213  
 1214  
 1215  
 1216  
 1217  
 1218  
 1219  
 1220  
 1221  
 1222  
 1223  
 1224  
 1225  
 1226  
 1227  
 1228  
 1229  
 1230  
 1231  
 1232  
 1233  
 1234  
 1235  
 1236  
 1237  
 1238  
 1239  
 1240  
 1241

**OURS-FAST:**

```

<think_perception></think_perception>
<answer_perception>```json\n{\n  \"bbox_2d\": [260, 112, 320, 220], \"label\": \"pedestrian\"}, {\n  \"bbox_2d\": [286, 130, 352, 184], \"label\": \"car\"\n}\n```</answer_perception>
<answer_prediction>```json\n{\n  \"bbox_2d\": [260, 112, 320, 220], \"future_action\": \"straight\"}, {\n  \"bbox_2d\": [286, 130, 352, 184], \"future_action\": \"straight\"\n}\n```</answer_prediction>
<think_planning> </think_planning>
<answer_planning>```json\n[{\n  \"point_2d\": [0.0, 0.0], \"label\": \"0.5s\"}, {\n  \"point_2d\": [0.0, 0.06], \"label\": \"1.0s\"}, {\n  \"point_2d\": [0.01, 0.33], \"label\": \"1.5s\"}, {\n  \"point_2d\": [0.01, 0.93], \"label\": \"2.0s\"}, {\n  \"point_2d\": [0.02, 1.81], \"label\": \"2.5s\"}, {\n  \"point_2d\": [0.03, 2.89], \"label\": \"3.0s\"\n}]\n```</answer_planning>
  
```

**OURS-DETAILED:**

Let's examine the image for key objects such as cars, buses, trucks, bicycles, pedestrians, and motorcycles. First, I notice a pedestrian on the left side of the image. I need to determine the bounding box coordinates for this pedestrian. The pedestrian appears to be standing on the sidewalk, so the bounding box should cover the area from the top of the head to the bottom of the feet. Next, I see a car on the right side of the image. It is smaller and further away, so the bounding box for this car will be smaller and positioned towards the center-right of the image. Now, let's determine the coordinates for each object:

1. Pedestrian: The pedestrian is on the left side of the image. The bounding box coordinates are approximately from (100, 120) to (200, 180).
2. Car: The car is on the right side of the image. The bounding box coordinates are approximately from (300, 150) to (400, 200). These coordinates are based on visual estimation from the image.

Let's compile this information into the required format.

```

</think_perception>
<answer_perception>
  {"bbox_2d": [258, 112, 318, 225], "label": "pedestrian"}, {"bbox_2d": [280, 132, 356, 183], "label": "car"}
</answer_perception>
  
```

**think\_prediction**

Let's analyze the future actions for each key object:

1. Pedestrian: The pedestrian is currently going straight and is not in the moving direction of the ego vehicle. The future state is also to go straight. Since the pedestrian is not affecting the ego vehicle, the future action remains "straight."
2. Car: The car is currently going straight and is in the moving direction of the ego vehicle. The future state is also to go straight. Since the car is not affecting the ego vehicle, the future action remains "straight."

Both objects are predicted to continue going straight as there are no indications of a change in their trajectory or behavior.

```

</think_prediction>
<answer_prediction>
  {"bbox_2d": [258, 112, 318, 225], "future_action": "straight"}, {"bbox_2d": [280, 132, 356, 183], "future_action": "straight"}
</answer_prediction>
  
```

**think\_planning**

Let's determine the planning trajectory for the ego vehicle:

1. Current Vehicle Speed: The ego vehicle is 0.0 m/s, and the historical trajectory shows a slight forward movement.
2. Ego Future Action: The ego vehicle is to go straight.
3. Trajectory Calculation:

The ego vehicle will accelerate from 0.0 m/s to a positive y-direction over the next 3 seconds. The trajectory points are calculated based on the acceleration and the time intervals.

4. Trajectory Points:

At 0.5s: The vehicle moves slightly forward, [0.0, 0.02]. At 1.0s: The vehicle moves further forward, [0.0, 0.17]. At 1.5s: The vehicle continues forward, [0.0, 0.44]. At 2.0s: The vehicle moves slightly to the right, [0.0, 1.13]. At 2.5s: The vehicle moves further forward, [0.01, 2.59]. At 3.0s: The vehicle moves slightly to the right, [0.01, 4.23].

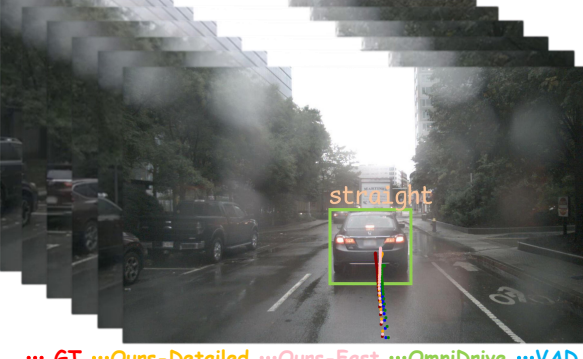
The trajectory reflects a gradual acceleration and forward movement.

```

</think_planning>
<answer_planning>
  {"point_2d": [0.0, 0.02], "label": "0.5s"}, {"point_2d": [0.0, 0.1], "label": "1.0s"}, {"point_2d": [0.0, 0.44], "label": "1.5s"}, {"point_2d": [0.0, 1.13], "label": "2.0s"}, {"point_2d": [0.01, 2.59], "label": "2.5s"}, {"point_2d": [0.01, 4.23], "label": "3.0s"}
</answer_planning>
  
```

**Figure 12: Visualization nuScenes cases with completed questions and answers. AutoDrive-P<sup>3</sup> successfully identifies and localizes the key objects, giving the correct actions. Based on these judgments, our method makes the efficiency planning decision in this sample.**

1242  
1243  
1244  
1245  
1246  
1247  
1248  
1249  
1250  
1251  
1252  
1253  
1254  
1255  
1256  
1257  
1258  
1259  
1260  
1261  
1262  
1263  
1264  
1265  
1266  
1267  
1268  
1269  
1270  
1271  
1272  
1273  
1274  
1275  
1276  
1277  
1278  
1279  
1280  
1281  
1282  
1283  
1284  
1285  
1286  
1287  
1288



```


1242  
1243  
1244  
1245  
1246  
1247  
1248  
1249  
1250  
1251  
1252  
1253  
1254  
1255  
1256  
1257  
1258  
1259  
1260  
1261  
1262  
1263  
1264  
1265  
1266  
1267  
1268  
1269  
1270  
1271  
1272  
1273  
1274  
1275  
1276  
1277  
1278  
1279  
1280  
1281  
1282  
1283  
1284  
1285  
1286  
1287  
1288


```

```


1242  
1243  
1244  
1245  
1246  
1247  
1248  
1249  
1250  
1251  
1252  
1253  
1254  
1255  
1256  
1257  
1258  
1259  
1260  
1261  
1262  
1263  
1264  
1265  
1266  
1267  
1268  
1269  
1270  
1271  
1272  
1273  
1274  
1275  
1276  
1277  
1278  
1279  
1280  
1281  
1282  
1283  
1284  
1285  
1286  
1287  
1288


```

```


1242  
1243  
1244  
1245  
1246  
1247  
1248  
1249  
1250  
1251  
1252  
1253  
1254  
1255  
1256  
1257  
1258  
1259  
1260  
1261  
1262  
1263  
1264  
1265  
1266  
1267  
1268  
1269  
1270  
1271  
1272  
1273  
1274  
1275  
1276  
1277  
1278  
1279  
1280  
1281  
1282  
1283  
1284  
1285  
1286  
1287  
1288


```

```


1242  
1243  
1244  
1245  
1246  
1247  
1248  
1249  
1250  
1251  
1252  
1253  
1254  
1255  
1256  
1257  
1258  
1259  
1260  
1261  
1262  
1263  
1264  
1265  
1266  
1267  
1268  
1269  
1270  
1271  
1272  
1273  
1274  
1275  
1276  
1277  
1278  
1279  
1280  
1281  
1282  
1283  
1284  
1285  
1286  
1287  
1288


```

```


1242  
1243  
1244  
1245  
1246  
1247  
1248  
1249  
1250  
1251  
1252  
1253  
1254  
1255  
1256  
1257  
1258  
1259  
1260  
1261  
1262  
1263  
1264  
1265  
1266  
1267  
1268  
1269  
1270  
1271  
1272  
1273  
1274  
1275  
1276  
1277  
1278  
1279  
1280  
1281  
1282  
1283  
1284  
1285  
1286  
1287  
1288


```

```


1242  
1243  
1244  
1245  
1246  
1247  
1248  
1249  
1250  
1251  
1252  
1253  
1254  
1255  
1256  
1257  
1258  
1259  
1260  
1261  
1262  
1263  
1264  
1265  
1266  
1267  
1268  
1269  
1270  
1271  
1272  
1273  
1274  
1275  
1276  
1277  
1278  
1279  
1280  
1281  
1282  
1283  
1284  
1285  
1286  
1287  
1288


```

1289  
1290  
1291  
1292  
1293  
1294  
1295

Figure 13: **Visualization nuScenes cases with completed questions and answers.** *AutoDrive-P<sup>3</sup>* successfully recognizes the driving command and provides the best trajectory instead of conservative one compared with other method.

```

1296 OURS-FAST:
1297 <think_perception></think_perception>
1298 <answer_perception>```json\n[{"bbox_2d": [17, 78, 153, 139], "label": "vehicle"}, {"bbox_2d": [316, 65, 367, 120], "label": "vehicle"}]\n```\n</answer_perception>
1299 <think_prediction></think_prediction>
1300 <answer_prediction>```json\n[{"bbox_2d": [17, 78, 153, 139], "future_position": "far, front"}, {"bbox_2d": [316, 65, 367, 120], "future_position": "far, front"}]\n```\n</answer_prediction>
1301 <think_planning></think_planning>
1302 <answer_planning>```json\n[{"x_y_radian": [5.28, 0.05, 0.02], "label": "0.5s"}, {"x_y_radian": [10.55, 0.15, 0.03], "label": "1.0s"}, {"x_y_radian": [15.75, 0.32, 0.04], "label": "1.5s"}, {"x_y_radian": [20.85, 0.55, 0.05], "label": "2.0s"}, {"x_y_radian": [25.75, 0.78, 0.05], "label": "2.5s"}, {"x_y_radian": [30.35, 1.01, 0.05], "label": "3.0s"}, {"x_y_radian": [34.55, 1.22, 0.05], "label": "3.5s"}, {"x_y_radian": [38.25, 1.39, 0.04], "label": "4.0s"}]\n```\n</answer_planning>
1303
1304
1305
1306
1307
1308
1309
1310
1311
1312
1313
1314
1315
1316
1317
1318
1319
1320
1321
1322
1323
1324
1325
1326
1327
1328
1329
1330
1331
1332
1333
1334
1335
1336
1337
1338
1339
1340
1341
1342
1343
1344
1345
1346
1347
1348
1349

```

```

1320 OURS-DETAILED:
1321 <think_perception>
1322 Let's analyze the image step by step to identify key objects and their coordinates:
1323 1. **Image Dimensions**: The image size is 672x168 pixels.
1324 2. **Vehicle Detection**: 
1325 - On the left side of the image, there is a vehicle visible on the road. Based on its position and size, it appears to be a car.
1326 - In the center-right portion of the image, another vehicle is present, likely a truck or SUV.
1327 - Coordinates: [13, 78, 152, 139], [316, 53, 369, 120]
1328 3. **Other Objects**: 
1329 - No pedestrians or bicycles are clearly visible in the image.
1330 - The background includes buildings, palm trees, and a Louis Vuitton store sign, but these are not categorized as key objects for the given question.
1331 4. **Final Output**: 
1332 <answer_perception>```json\n[{"bbox_2d": [13, 78, 152, 139], "label": "vehicle"}, {"bbox_2d": [316, 53, 369, 120], "label": "vehicle"}]\n```\n</answer_perception>
1333 <answer_prediction>```json\n[{"bbox_2d": [13, 78, 152, 139], "future_position": "far, front"}, {"bbox_2d": [316, 53, 369, 120], "future_position": "far, front"}]\n```\n</answer_prediction>
1334 <think_planning>
1335 1. **Ego Vehicle State**: 
1336 - Current velocity (vx): 10.85 m/s, vy: -0.21 m/s, ax: 0.20 m/s2, ay: 0.27 m/s2.
1337 - Driving Command: GO STRAIGHT.
1338 - Historical Trajectory: The ego vehicle has been moving forward with a slight leftward yaw angle, indicating a minor leftward trajectory over the past 1.5 seconds.
1339 2. **Key Object Considerations**: 
1340 - **Vehicle on the Left**: This vehicle is predicted to move forward and slightly to the left. The ego vehicle must maintain a safe distance to avoid collision.
1341 - **Vehicle Ahead**: This vehicle is also predicted to move forward along its current path. The ego vehicle should continue straight to avoid any potential collision.
1342 3. **Planning Points (Every 0.5s)**: 
1343 - **0.5s**: The ego vehicle moves forward with a slight leftward yaw angle. The vehicle on the left is still to the left of the ego vehicle's path, so no adjustment is needed.
1344 - **1.0s**: The ego vehicle continues straight with a slight leftward yaw angle. The vehicle ahead remains in the center-right lane, so no adjustment is needed.
1345 - **1.5s**: The ego vehicle maintains its trajectory with a slight leftward yaw angle. The vehicle on the left is still to the left of the ego vehicle's path, so no adjustment is needed.
1346 - **2.0s**: The ego vehicle continues straight with a slight leftward yaw angle. The vehicle ahead remains in the center-right lane, so no adjustment is needed.
1347 - **2.5s**: The ego vehicle maintains its trajectory with a slight leftward yaw angle. The vehicle on the left is still to the left of the ego vehicle's path, so no adjustment is needed.
1348 - **3.0s**: The ego vehicle continues straight with a slight leftward yaw angle. The vehicle ahead remains in the center-right lane, so no adjustment is needed.
1349 - **3.5s**: The ego vehicle maintains its trajectory with a slight leftward yaw angle. The vehicle on the left is still to the left of the ego vehicle's path, so no adjustment is needed.
1350 - **4.0s**: The ego vehicle continues straight with a slight leftward yaw angle. The vehicle ahead remains in the center-right lane, so no adjustment is needed.
1351 4. **Conclusion**: The ego vehicle can continue moving straight with a slight leftward yaw angle, as there are no immediate collision risks with the key objects. The trajectory is adjusted minimally to maintain a safe distance from the vehicle on the left while continuing to follow the driving command of going straight.
1352 </think_planning>
1353
1354
1355
1356
1357
1358
1359
1360
1361
1362
1363
1364
1365
1366
1367
1368
1369
1370
1371
1372
1373
1374
1375
1376
1377
1378
1379
1380
1381
1382
1383
1384
1385
1386
1387
1388
1389
1390
1391
1392
1393
1394
1395
1396
1397
1398
1399
1400
1401
1402
1403
1404
1405
1406
1407
1408
1409
1410
1411
1412
1413
1414
1415
1416
1417
1418
1419
1420
1421
1422
1423
1424
1425
1426
1427
1428
1429
1430
1431
1432
1433
1434
1435
1436
1437
1438
1439
1440
1441
1442
1443
1444
1445
1446
1447
1448
1449
1450
1451
1452
1453
1454
1455
1456
1457
1458
1459
1460
1461
1462
1463
1464
1465
1466
1467
1468
1469
1470
1471
1472
1473
1474
1475
1476
1477
1478
1479
1480
1481
1482
1483
1484
1485
1486
1487
1488
1489
1490
1491
1492
1493
1494
1495
1496
1497
1498
1499
1500
1501
1502
1503
1504
1505
1506
1507
1508
1509
1510
1511
1512
1513
1514
1515
1516
1517
1518
1519
1520
1521
1522
1523
1524
1525
1526
1527
1528
1529
1530
1531
1532
1533
1534
1535
1536
1537
1538
1539
1540
1541
1542
1543
1544
1545
1546
1547
1548
1549
1550
1551
1552
1553
1554
1555
1556
1557
1558
1559
1560
1561
1562
1563
1564
1565
1566
1567
1568
1569
1570
1571
1572
1573
1574
1575
1576
1577
1578
1579
1580
1581
1582
1583
1584
1585
1586
1587
1588
1589
1590
1591
1592
1593
1594
1595
1596
1597
1598
1599
1600
1601
1602
1603
1604
1605
1606
1607
1608
1609
1610
1611
1612
1613
1614
1615
1616
1617
1618
1619
1620
1621
1622
1623
1624
1625
1626
1627
1628
1629
1630
1631
1632
1633
1634
1635
1636
1637
1638
1639
1640
1641
1642
1643
1644
1645
1646
1647
1648
1649
1650
1651
1652
1653
1654
1655
1656
1657
1658
1659
1660
1661
1662
1663
1664
1665
1666
1667
1668
1669
1670
1671
1672
1673
1674
1675
1676
1677
1678
1679
1680
1681
1682
1683
1684
1685
1686
1687
1688
1689
1690
1691
1692
1693
1694
1695
1696
1697
1698
1699
1700
1701
1702
1703
1704
1705
1706
1707
1708
1709
1710
1711
1712
1713
1714
1715
1716
1717
1718
1719
1720
1721
1722
1723
1724
1725
1726
1727
1728
1729
1730
1731
1732
1733
1734
1735
1736
1737
1738
1739
1740
1741
1742
1743
1744
1745
1746
1747
1748
1749
1750
1751
1752
1753
1754
1755
1756
1757
1758
1759
1760
1761
1762
1763
1764
1765
1766
1767
1768
1769
1770
1771
1772
1773
1774
1775
1776
1777
1778
1779
1780
1781
1782
1783
1784
1785
1786
1787
1788
1789
1790
1791
1792
1793
1794
1795
1796
1797
1798
1799
1800
1801
1802
1803
1804
1805
1806
1807
1808
1809
1810
1811
1812
1813
1814
1815
1816
1817
1818
1819
1820
1821
1822
1823
1824
1825
1826
1827
1828
1829
1830
1831
1832
1833
1834
1835
1836
1837
1838
1839
1840
1841
1842
1843
1844
1845
1846
1847
1848
1849
1850
1851
1852
1853
1854
1855
1856
1857
1858
1859
1860
1861
1862
1863
1864
1865
1866
1867
1868
1869
1870
1871
1872
1873
1874
1875
1876
1877
1878
1879
1880
1881
1882
1883
1884
1885
1886
1887
1888
1889
1890
1891
1892
1893
1894
1895
1896
1897
1898
1899
1900
1901
1902
1903
1904
1905
1906
1907
1908
1909
1910
1911
1912
1913
1914
1915
1916
1917
1918
1919
1920
1921
1922
1923
1924
1925
1926
1927
1928
1929
1930
1931
1932
1933
1934
1935
1936
1937
1938
1939
1940
1941
1942
1943
1944
1945
1946
1947
1948
1949
1950
1951
1952
1953
1954
1955
1956
1957
1958
1959
1960
1961
1962
1963
1964
1965
1966
1967
1968
1969
1970
1971
1972
1973
1974
1975
1976
1977
1978
1979
1980
1981
1982
1983
1984
1985
1986
1987
1988
1989
1990
1991
1992
1993
1994
1995
1996
1997
1998
1999
2000
2001
2002
2003
2004
2005
2006
2007
2008
2009
2010
2011
2012
2013
2014
2015
2016
2017
2018
2019
2020
2021
2022
2023
2024
2025
2026
2027
2028
2029
2030
2031
2032
2033
2034
2035
2036
2037
2038
2039
2040
2041
2042
2043
2044
2045
2046
2047
2048
2049
2050
2051
2052
2053
2054
2055
2056
2057
2058
2059
2060
2061
2062
2063
2064
2065
2066
2067
2068
2069
2070
2071
2072
2073
2074
2075
2076
2077
2078
2079
2080
2081
2082
2083
2084
2085
2086
2087
2088
2089
2090
2091
2092
2093
2094
2095
2096
2097
2098
2099
2100
2101
2102
2103
2104
2105
2106
2107
2108
2109
2110
2111
2112
2113
2114
2115
2116
2117
2118
2119
2120
2121
2122
2123
2124
2125
2126
2127
2128
2129
2130
2131
2132
2133
2134
2135
2136
2137
2138
2139
2140
2141
2142
2143
2144
2145
2146
2147
2148
2149
2150
2151
2152
2153
2154
2155
2156
2157
2158
2159
2160
2161
2162
2163
2164
2165
2166
2167
2168
2169
2170
2171
2172
2173
2174
2175
2176
2177
2178
2179
2180
2181
2182
2183
2184
2185
2186
2187
2188
2189
2190
2191
2192
2193
2194
2195
2196
2197
2198
2199
2200
2201
2202
2203
2204
2205
2206
2207
2208
2209
2210
2211
2212
2213
2214
2215
2216
2217
2218
2219
2220
2221
2222
2223
2224
2225
2226
2227
2228
2229
2230
2231
2232
2233
2234
2235
2236
2237
2238
2239
2240
2241
2242
2243
2244
2245
2246
2247
2248
2249
2250
2251
2252
2253
2254
2255
2256
2257
2258
2259
2260
2261
2262
2263
2264
2265
2266
2267
2268
2269
2270
2271
2272
2273
2274
2275
2276
2277
2278
2279
2280
2281
2282
2283
2284
2285
2286
2287
2288
2289
2290
2291
2292
2293
2294
2295
2296
2297
2298
2299
2300
2301
2302
2303
2304
2305
2306
2307
2308
2309
2310
2311
2312
2313
2314
2315
2316
2317
2318
2319
2320
2321
2322
2323
2324
2325
2326
2327
2328
2329
2330
2331
2332
2333
2334
2335
2336
2337
2338
2339
2340
2341
2342
2343
2344
2345
2346
2347
2348
2349
2350
2351
2352
2353
2354
2355
2356
2357
2358
2359
2360
2361
2362
2363
2364
2365
2366
2367
2368
2369
2370
2371
2372
2373
2374
2375
2376
2377
2378
2379
2380
2381
2382
2383
2384
2385
2386
2387
2388
2389
2390
2391
2392
2393
2394
2395
2396
2397
2398
2399
2400
2401
2402
2403
2404
2405
2406
2407
2408
2409
2410
2411
2412
2413
2414
2415
2416
2417
2418
2419
2420
2421
2422
2423
2424
2425
2426
2427
2428
2429
2430
2431
2432
2433
2434
2435
2436
2437
2438
2439
2440
2441
2442
2443
2444
2445
2446
2447
2448
2449
2450
2451
2452
2453
2454
2455
2456
2457
2458
2459
2460
2461
2462
2463
2464
2465
2466
2467
2468
2469
2470
2471
2472
2473
2474
2475
2476
2477
2478
2479
2480
2481
2482
2483
2484
2485
2486
2487
2488
2489
2490
2491
2492
2493
2494
2495
2496
2497
2498
2499
2500
2501
2502
2503
2504
2505
2506
2507
2508
2509
2510
2511
2512
2513
2514
2515
2516
2517
2518
2519
2520
2521
2522
2523
2524
2525
2526
2527
2528
2529
2530
2531
2532
2533
2534
2535
2536
2537
2538
2539
2540
2541
2542
2543
2544
2545
2546
2547
2548
2549
2550
2551
2552
2553
2554
2555
2556
2557
2558
2559
2560
2561
2562
2563
2564
2565
2566
2567
2568
2569
2570
2571
2572
2573
2574
2575
2576
2577
2578
2579
2580
2581
2582
2583
2584
2585
2586
2587
2588
2589
2590
2591
2592
2593
2594
2595
2596
2597
2598
2599
2600
2601
2602
2603
2604
2605
2606
2607
2608
2609
2610
2611
2612
2613
2614
2615
2616
2617
2618
2619
2620
2621
2622
2623
2624
2625
2626
2627
2628
2629
2630
2631
2632
2633
2634
2635
2636
2637
2638
2639
2640
2641
2642
2643
2644
2645
2646
2647
2648
2649
2650
2651
2652
2653
2654
2655
2656
2657
2658
2659
2660
2661
2662
2663
2664
2665
2666
2667
2668
2669
2670
2671
2672
2673
2674
2675
2676
2677
2678
2679
2680
2681
2682
2683
2684
2685
2686
2687
2688
2689
2690
2691
2692
2693
2694
2695
2696
2697
2698
2699
2700
2701
2702
2703
2704
2705
2706
2707
2708
2709
2710
2711
2712
2713
2714
2715
2716
2717
2718
2719
2720
2721
2722
2723
2724
2725
2726
2727
2728
2729
2730
2731
2732
2733
2734
2735
2736
2737
2738
2739
2740
2741
2742
2743
2744
2745
2746
2747
2748
2749
2750
2751
2752
2753
2754
2755
2756
2757
2758
2759
2760
2761
2762
2763
2764
2765
2766
2767
2768
2769
2770
2771
2772
2773
2774
2775
2776
2777
2778
2779
2780
2781
2782
2783
2784
2785
2786
2787
2788
2789
2790
2791
2792
2793
2794
2795
2796
2797
2798
2799
2800
2801
2802
2803
2804
2805
2806
2807
2808
2809
2810
2811
2812
2813
2814
2815
2816
2817
2818
2819
2820
2821
2822
2823
2824
2825
2826
2827
2828
2829
2830
2831
2832
2833
2834
2835
2836
2837
2838
2839
2840
2841
2842
2843
2844
2845
2846
2847
2848
2849
2850
2851
2852
2853
2854
2855
2856
2857
2858
2859
2860
2861
2862
2863
2864
2865
2866
2867
2868
2869
2870
2871
2872
2873
2874
2875
2876
2877
2878
2879
2880
2881
2882
2883
2884
2885
2886
2887
2888
2889
2890
2891
2892
2893
2894
2895
2896
2897
2898
2899
2900
2901
2902
2903
2904
2905
2906
2907
2908
2909
2910
2911
2912
2913
2914
2915
2916
2917
2918
2919
2920
2921
2922
2923
2924
2925
2926
2927
2928
2929
2930
2931
2932
2933
2934
2935
2936
2937
2938
2939
2940
2941
2942
2943
2944
2945
2946
2947
2948
2949
2950
2951
2952
2953
2954
2955
2956
2957
2958
2959
2960
2961
2962
2963
2964
2965
2966
2967
2968
2969
2970
2971
2972
2973
2974
2975
2976
2977
2978
2979
2980
2981
2982
2983
2984
2985
2986
2987
2988
2989
2990
2991
2992
2993
2994
2995
2996
2997
2998
2999
2999

```

Figure 14: **Visualization NAVSIM cases with completed questions and answers.** *AutoDrive-P<sup>3</sup>* successfully predicts the future action of the truck and follows the forward vehicle in a safe distance.

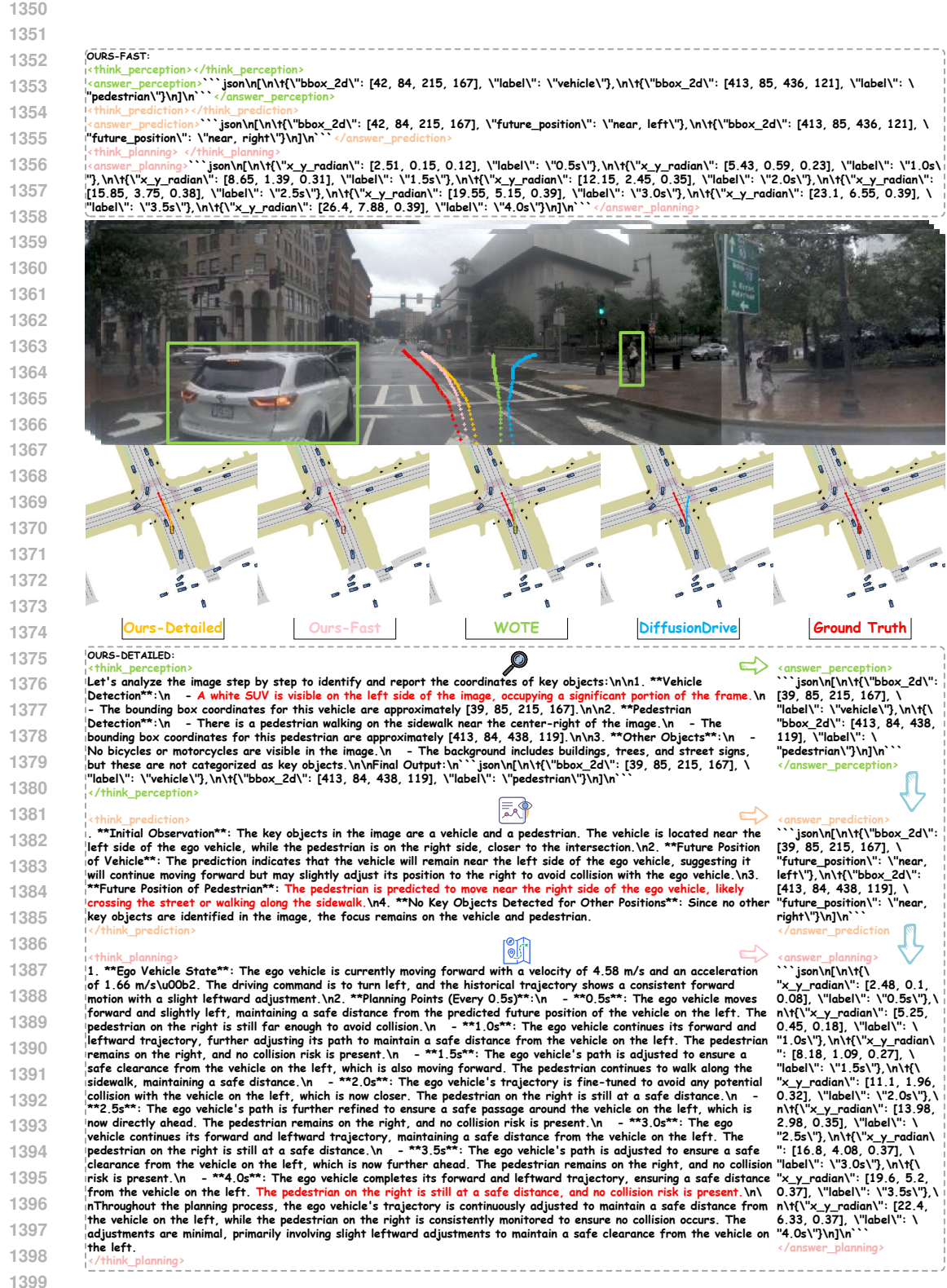


Figure 15: **Visualization NAVSIM cases with completed questions and answers.** *AutoDrive-P<sup>3</sup>* successfully locates the key object on the left and take a appropriate lane change action to move forward, while other methods provide a wrong trajectories to turn right.

```

1404 OURS-FAST:
1405 <think_perception></think_perception>
1406 <answer_perception> ````json\n[{\\"bbox_2d\": [0, 74, 175, 167], \"label\": \"vehicle\"}, {\\"bbox_2d\": [162, 88, 246, 162], \"label\": \"vehicle\"}, {\\"bbox_2d\": [455, 76, 493, 122], \"label\": \"pedestrian\"}]\n````</answer_perception>
1407 <think_prediction></think_prediction>
1408 <answer_prediction> ````json\n[{\\"bbox_2d\": [0, 74, 175, 167], \"future_position\": \"near, left\"}, {\\"bbox_2d\": [162, 88, 246, 162], \"future_position\": \"far, left\"}, {\\"bbox_2d\": [455, 76, 493, 122], \"future_position\": \"near, right\"}]\n````</answer_prediction>
1409 <think_planning></think_planning>
1410 <answer_planning> ````json\n[{\\"x_y_radian\": [2.51, 0.11, 0.1], \"label\": \"0.5s\"}, {\\"x_y_radian\": [3.53, 0.51, 0.19], \"label\": \"1.0s\"}, {\\"x_y_radian\": [8.51, 1.15, 0.23], \"label\": \"1.5s\"}, {\\"x_y_radian\": [11.98, 1.95, 0.25], \"label\": \"2.0s\"}, {\\"x_y_radian\": [15.75, 2.89, 0.27], \"label\": \"2.5s\"}, {\\"x_y_radian\": [19.79, 3.95, 0.28], \"label\": \"3.0s\"}, {\\"x_y_radian\": [23.95, 5.09, 0.29], \"label\": \"3.5s\"}, {\\"x_y_radian\": [28.1, 6.25, 0.29], \"label\": \"4.0s\"]}\n````</answer_planning>
1411
1412
1413
1414
1415
1416
1417
1418
1419

1420
1421
1422
1423
1424
1425
1426

1427 OURS-DETAILED:
1428 <think_perception>
1429 Let's analyze the image step by step to identify and report the coordinates of key objects:
1430 n1. **Vehicle Detection**: The image shows a black vehicle on the left side of the frame. It appears to be a van or SUV. In - Coordinates: [0, 70, 175, 167] - Another vehicle is visible further down the road, closer to the center. In - Coordinates: [160, 87, 246, 162]. **Pedestrian Detection**: A pedestrian is walking on the sidewalk on the right side of the frame. In - Coordinates: [456, 77, 493, 121]. **Other Objects**: There are no bicycles or motorcycles visible in the image. In - The background includes buildings and traffic lights, but these are not categorized as key objects. In - Final Output: ````json\n[{\\"bbox_2d\": [0, 70, 175, 167], \"label\": \"vehicle\"}, {\\"bbox_2d\": [160, 87, 246, 162], \"label\": \"vehicle\"}, {\\"bbox_2d\": [456, 77, 493, 121], \"label\": \"pedestrian\"}]\n````</think_perception>
1431 <think_prediction>
1432 1. **Initial Observation**: The key objects in the image include a black vehicle on the left, another vehicle further ahead and to the left, and a pedestrian on the right side of the street. In - **Future Position of Key Objects**:
1433 n1. - The black vehicle is predicted to move near and to the left of its current position. In - The vehicle ahead and to the left is also predicted to move near and to the left. In - The pedestrian is predicted to move near and to the right. In n2. **Reasoning**: Given the current positions and the predicted movement paths, the black vehicle and the vehicle ahead are likely to continue moving forward with a slight leftward trajectory. The pedestrian is expected to move along the sidewalk to the right.
1434 </think_prediction>
1435 <think_planning>
1436 1. **Ego Vehicle State**: The ego vehicle is currently moving forward with a velocity of 4.72 m/s and an acceleration of 0.27 m/s2. The driving command is to turn left. In 2. **Historical Trajectory**: The historical trajectory shows a consistent forward motion with a slight leftward adjustment over time. In 3. **Future Planning Points**:
1437 n1. - **0.5s**: The ego vehicle will continue moving forward while initiating a left turn. The pedestrian is to the right, so no immediate collision risk exists. The black vehicle ahead is also moving forward, maintaining a safe distance. In - **1.0s**: The ego vehicle continues its left turn, increasing the yaw angle. The pedestrian remains to the right, and the black vehicle ahead is still at a safe distance. The trajectory adjustment ensures no collision with the pedestrian. In - **1.5s**: The ego vehicle further executes the left turn, with the yaw angle increasing. The pedestrian is now further to the right, and the black vehicle ahead maintains a safe distance. The trajectory is adjusted to ensure a smooth turn without collision. In - **2.0s**: The ego vehicle continues the left turn, with the yaw angle approaching 0.3 radians. The pedestrian is now significantly to the right, and the black vehicle ahead is still at a safe distance. The trajectory is fine-tuned to avoid any potential collision. In - **2.5s**: The ego vehicle maintains the left turn, with the yaw angle at 0.33 radians. The pedestrian is now even further to the right, and the black vehicle ahead is still at a safe distance. The trajectory is adjusted to ensure a smooth and safe turn. In - **3.0s**: The ego vehicle continues the left turn, with the yaw angle at 0.34 radians. The pedestrian is now at a considerable distance to the right, and the black vehicle ahead is still at a safe distance. The trajectory is fine-tuned to ensure a smooth turn. In - **3.5s**: The ego vehicle maintains the left turn, with the yaw angle at 0.34 radians. The pedestrian is now at a significant distance to the right, and the black vehicle ahead is still at a safe distance. The trajectory is adjusted to ensure a smooth turn. In - **4.0s**: The ego vehicle completes the left turn, with the yaw angle at 0.34 radians. The pedestrian is now at a considerable distance to the right, and the black vehicle ahead is still at a safe distance. The trajectory is finalized to ensure a smooth and safe turn. In 4. **Collision Avoidance**: Throughout the planning process, the ego vehicle's trajectory is adjusted to maintain a safe distance from the pedestrian and the black vehicle ahead. The left turn is executed smoothly, with continuous monitoring of the pedestrian's position to ensure no collision occurs. In 5. **Final Adjustment**: The final trajectory ensures a safe and smooth left turn, avoiding any potential collisions with the pedestrian and the black vehicle ahead. The trajectory is optimized to maintain a safe distance and execute the driving command effectively.
1438 </think_planning>
1439
1440
1441
1442
1443
1444
1445
1446
1447
1448
1449
1450
1451
1452
1453
1454
1455
1456
1457

```

Figure 16: **Visualization NAVSIM cases with completed questions and answers.** *AutoDrive-P<sup>3</sup>* successfully locates key objects on the left and take a appropriate lane change action to move forward, while other methods drive into an illegal driving area.

```

1458 OURS-FAST:
1459 <think_perception></think_perception>
1460 <answer_perception>```json\n\n\t("bbox_2d": [], "label": []]\n```</answer_perception>
1461 <think_prediction></think_prediction>
1462 <answer_prediction>```json\n\n\t("bbox_2d": [], "future_position": []]\n```</answer_prediction>
1463 <think_planning></think_planning>
1464 <answer_planning>```json\n\n\t("x_y_radian": [1.35, 0.0, 0.0], "label": "\0.5s"),\n\t("x_y_radian": [3.15, -0.02, -0.02], "label": "\1.0s"),
1465 \n\t("x_y_radian": [5.25, -0.11, -0.08], "label": "\1.5s"),\n\t("x_y_radian": [7.55, -0.41, -0.19], "label": "\2.0s"),
1466 \n\t("x_y_radian": [9.89, -1.02, -0.35], "label": "\2.5s"),\n\t("x_y_radian": [12.1, -2.05, -0.55], "label": "\3.0s"),
1467 \n\t("x_y_radian": [13.98, -3.51, -0.78], "label": "\3.5s"),\n\t("x_y_radian": [15.42, -5.35, -1.02], "label": "\4.0s")
1468 ````</answer_planning>
1469
1470
1471
1472
1473
1474
1475
1476
1477
1478
1479
1480
1481
1482
1483
1484
1485
1486
1487
1488
1489
1490
1491
1492
1493
1494
1495
1496
1497
1498
1499
1500
1501
1502
1503
1504
1505
1506
1507
1508
1509
1510
1511

```

```

<answer_perception>
```json\n\n\t("bbox_2d": [], "label": []]\n```</answer_perception>
<answer_prediction>
```json\n\n\t("bbox_2d": [], "future_position": []]\n```</answer_prediction>
<answer_planning>
```json\n\n\t("x_y_radian": [1.36, 0.0, -0.01], "label": "\0.5s"),
\t("x_y_radian": [3.08, -0.03, -0.04], "label": "\1.0s"),
\t("x_y_radian": [5.06, -0.16, -0.12], "label": "\1.5s"),
\t("x_y_radian": [7.15, -0.5, -0.25], "label": "\2.0s"),
\t("x_y_radian": [9.2, -1.2, -0.43], "label": "\2.5s"),
\t("x_y_radian": [11.1, -2.3, -0.63], "label": "\3.0s"),
\t("x_y_radian": [12.78, -3.78, -0.83], "label": "\3.5s"),
\t("x_y_radian": [14.15, -5.65, -1.03], "label": "\4.0s")
```</answer_planning>

```

Figure 17: **Visualization NAVSIM cases with completed questions and answers.** *AutoDrive-P<sup>3</sup>* successfully recognizes the “Turn Right” command and provide the right planning trajectory, while other methods drive towards the building leading to collisions.

1512 F PROMPTS  
15131514 In this section, we provide the completed and specific prompts used in the training/inference and  
1515 prompts used to generate  $P^3$ -CoT dataset. The prompt used in the training/inference is as follows.  
1516

```

1517 You are an expert driving assistant. As an expert driving assistant,
1518 analyze the 3-second driving video context and answer the perception,
1519 prediction and planning question in the final frame.
1520 Output format is '<think_perception> </think_perception>\n<
1521 answer_perception> </answer_perception>\n<think_prediction> </
1522 think_prediction>\n<answer_prediction> </answer_prediction>\n<
1523 think_planning> </think_planning>\n<answer_planning> </
1524 answer_planning>'.
1525 Output the step-by-step Chain-of-Thought (CoT) reasoning process in <
1526 think> </think> tags and final answer in <answer> </answer> tags,
1527 respectively.
1528 Ego Future Action is [Ego_Future_Action]. You current vehicle speed is [
1529 VEHICLE_SPEED] m/s, and the historical trajectory of the ego vehicle
1530 is [HISTORICAL_TRAJECTORY].
```

1529  
1530 To sufficiently extract knowledge from Qwen2.5-VL-72B, we ask Qwen2.5-VL-72B to output the  
1531 Chain-of-Thought (CoT) step by step. Qwen2.5-VL-72B is also required to use the CoT of perception  
1532 tasks when it generates the CoT of prediction, and use the CoT of perception and prediction  
1533 tasks when it generates the CoT of planning.

```

1534 # Perception CoT
1535 PROMPT_FORMAT = """I will provide you with a final frame image of video,
1536 an original question, and its answer related to the image. Your task
1537 is to answer it requires step-by-step Chain-of-Thought (CoT)
1538 reasoning with numerical or mathematical expressions where applicable
1539 . The reasoning process can include expressions like "let me think,"
1540 "oh, I see," or other natural language thought expressions.
1541 Input Format:
1542 Original Question: {original_question}
1543 Original Answer: {original_answer}
1544 Output Format:
1545 <think>step-by-step reasoning process</think>
1546 <answer>easy to verify answer</answer>
1547 """
1548 QUESTION = "Examine the final frame image of video for key objects and
1549 report the coordinates of each detected object. Key object categories
1550 include: car, bus, truck, bicycle, pedestrian, motorcycle. The image
1551 size is 896x504."
1552 ANSWER_FORMAT = "[\n\t{\\"bbox_2d\\": {bbox}, \"label\": \"{label}\\"}\n]"
1553
1554 # Prediction and Planning
1555 PROMPT_FORMAT = """I will provide you with a final frame image of video,
1556 the key objects in this frame, an question, a video Context, vehicle
1557 speed, historical trajectory (last 3 seconds) and its prediction and
1558 planning answer. Your task is to answer it requires step-by-step
1559 Chain-of-Thought (CoT) reasoning with numerical or mathematical
1560 expressions where applicable. The reasoning process can include
1561 expressions like "let me think," "oh, I see," or other natural
1562 language thought expressions.
1563 Note that prediction and planning answers are the next 3-second future
1564 action for each object and ego vehicle planning trajectory. Video
1565 context is the 3-second context.
1566 Input Format:
1567 Key Objects: {key_objs}
1568 Question: {original_question}
1569 Video Context: {original_thinking}
1570 Current Vehicle Speed: {vehicle_speed} m/s
1571 Historical Trajectory (last 3 seconds, meters): {Historical_Trajectory}
1572 Prediction Answer: \n{original_answer_prediction}
```

```

1566 Planning Answer: \n{original_answer_planning}
1567 Output Format:
1568 <think_prediction>step-by-step prediction reasoning process</
1569   think_prediction>
1570 <answer_prediction>easy to verify prediction answer</answer_prediction>
1571 <think_planning>step-by-step planning reasoning process</think_planning>
1572 <answer_planning>easy to verify planning answer</answer_planning>
1573 """
1574 QUESTION = """Predict the future action for each object and give the the
1575   ego vehicle planning trajectory. Future action can be: stop, straight
1576   , right, left. Planning trajectory is 6 points in the next 3 seconds
1577   (each point means 0.5s).
1578 Please use the format as [x, y] in meters, where x-axis is perpendicular,
1579   and y-axis is parallel to the direction you are facing.
1580 If y > 0, it means that the ego is to GO STRAIGHT, and vice versa.
1581 If x > 0, it means that the ego is to TURN RIGHT, and vice versa.
1582 Note that current Vehicle Speed does affect the ego vehicle planning
1583   trajectory but you also should consider Historical Trajectory, Key
1584   Objects' Prediction Answers, Ego Action and the Video Context.
1585 Uing numerical or mathematical expressions where applicable.
1586 """
1587
1588
1589
1590
1591
1592
1593
1594
1595
1596
1597
1598
1599
1600
1601
1602
1603
1604
1605
1606
1607
1608
1609
1610
1611
1612
1613
1614
1615
1616
1617
1618
1619

```